Title

The Role of Wnt Signaling Proteins in Neurodevelopement and Psychiatry

Permalink

https://escholarship.org/uc/item/3xm9k6fn

Author

Stanley, Robert

Publication Date

2016

Peer reviewed|Thesis/dissertation

The Role of Wnt Signaling Proteins in Neurodevelopment and

Psychiatry

by

Robert Stanley

DISSERTATION

Submitted in partial satisfaction of the requirements for the degree of

DOCTOR OF PHILOSOPHY

in

Cell Biology

Acknowledgements

I would first like to thank my graduate advisor Ben Cheyette whose mentorship has been invaluable to me as a graduate student. I initially had difficulties as a graduate student and other PIs may have been hesitant to accept me in their lab, but Ben has always been very supportive of me and my efforts and encouraged me to continue in my graduate career. I will always be grateful to him for making graduate school a good experience, for creating a wonderful working environment and for having faith in me. I would also like to thank my thesis committee members John Rubenstein and Vikaas Sohal for their input and the help of their labs in completing this project.

I would like to thank all of the members of the Cheyette lab. Nathan Okerlund and Annie Arguello were graduate students and my initial mentors when I started in lab and taught me many of the techniques I learned. They continued to be helpful throughout my first years in the lab. Pierre-Marie Martin and XiaoYong Yang have been postdocs in the lab for most of my tenure here and have always been most helpful whenever I needed their expertise and advice. Previous and current postdocs that have been helpful and contributed to my project were Saul Kivimae, Kim Mulligan, Adam Ross, and Andiara E. Freitas. I'd like to thank our lab manager Petros Minasi for his invaluable help over the years. I would also like to thank Dan Vogt and Emily Pai from the Rubenstein lab for their help in the completion of this project.

I would like to thank my friends and family who have always been supportive of me and encouraged me to do well and persevere. My mother Irene, my sister Tammie, and my grandparents Alice and Roque have always been loving and supportive over the years. Several classmates have been good friends to me over the years and been very

The Role of Wnt Signaling Proteins in Neurodevelopment and Psychiatric Susceptibility

Robert Stanley

Abstract

Proper regulation of cell signaling pathways is required for normal neurodevelopment. Dysfunction in signaling can lead to problems in the development of the brain and increased susceptibility to develop psychiatric disorders. Many components are required to act in concert in multiple intersecting pathways, and mutations in these components can lead to aberrant signaling. Modern human genetics is increasingly identifying genes and gene mutations associated with psychiatric risk via genome-wide sequencing of patients with psychiatric disorders. Once specific genes and their mutations are identified as possible contributors to disease, experimental assays are required to determine the functionality of these genes and their variants in neurodevelopment and signaling.

The scaffolding protein Dix-Domain Containing 1 (Dixdc1) is a positive regulator of Wnt-/β-catenin signaling that interacts with the psychiatric risk gene Disrupted in Schizophrenia 1 (Disc1). We have a utilized a Dixdc1 knock-out mouse line to help determine functions of this gene in neurodevelopment. Using cultured hippocampal neurons and tissue sections from intact brains expressing GFP in cortical neurons, we have interrogated what effect deletion of Dixdc1 has on the development of dendrites, dendritic spines, and synapses in pyramidal neurons of the forebrain. In addition, using sequencing data from patient samples of three different psychiatric disorders (ASD,

Schizophrenia, and Bipolar Disorder) we have identified a set of rare missense mutations in the Dixdc1 locus that are present in patients with these diseases. These variants were then functionally tested using several neurodevelopmental and canonical Wnt/Beta-catenin signaling assays.

Our results show that Dixdc1 is required for proper development of spines- both in their quantity and maturation- and excitatory synapses in forebrain pyramidal neurons. There appears to be no effect on dendrite complexity (in a mixed genetic background) or on inhibitory synapse numbers. Additionally, mutant versions of Dixdc1 found in ASD patient samples that have aberrant Wnt signaling are unable to rescue neurodevelopmental phenotypes in KO neurons, while some of these variants that are hyperactive for Wnt/β-catenin signaling have dominant negative effects when expressed in wild type neurons.

Table of Contents

List of Figures and Tables

Chapter 1

Introduction

Neurodevelopment and Wnt Signaling

Neurodevelopment is a highly regulated process involving multiple intersecting signaling pathways. Disruptions in these pathways can lead to defective neurodevelopment, resulting in defects ranging from severe neural malformation to various psychiatric disorders. Understanding how these signaling pathways function in proper neurodevelopment is key to elucidating the pathogenesis of neurological and psychiatric diseases. Modern genomics is aiding in this discovery by identifying genes and mutations in these genes that contribute to disease etiology. When a gene is identified, experimental assays are required to determine what role it plays in the normal function of a signaling pathway and what effect that has in development.

One of the key signaling pathways critical to neurodevelopment is Wnt signaling, composed of several separate and intersecting signaling pathways. These pathways are highly conserved in all mulitcellular animals. There are 19 different Wnt proteins in humans and various receptors employed in several branching pathways that use Wnts as ligands. The best described of these is the "canonical" Wnt/β-catenin pathway in which a Wnt ligand binds to a Frizzled/LRP co-receptor complex which in turn leads to inhibition of the β-catenin degradation complex. The degradation complex is composed of several components including Axin, adenomatosis polyposis coli (APC), and glycogen synthase kinase 3 (GSK3), as well as others (Logan et al., 2004). In the absence of a Wnt signal this complex binds and phosphorylates β-catenin, targeting it

1

for ubiquitination and degradation by the proteasome. When Wnt binds the Frizzled/LRP receptor complex, the degradation complex is disrupted. Disheveled (Dvl) and Axin translocate to the receptor complex and GSK phosphorylation of β-catenin is reduced. This leads to an accumulation of cytosolic β-catenin, which then translocates to the nucleus where it interacts with T-cell factor/lymphoid enhancing factor (TCF/LEF) transcription factors, to alter transcription of various target proteins. In the brain this pathway plays a role in regulating cell proliferation and specification (Okerlund et al., 2011). It is also critical for establishing brain regionalization along the anterior-posterior axis (Kiecker et al., 2001).

Additional "non-canonical" (i.e. non-β-catenin dependent) Wnt pathways include the planar cell polarity (PCP) pathway and the Wnt/Calcium pathway. The PCP pathway plays a role in regulating aspects of neurodevelopment including convergent extension movements involved in the formation of the neural tube, as well as cell migration, dendrite and spine maturation, and axon guidance (Mulligan et al., 2012). In PCP signaling in mammals, Wnt binds to Frizzled receptors and activates the pathway via Dvl. Several intermediate proteins are involved in the transduction of the pathway which leads to regulation of transverse cell polarity through the cytoskeleton. Downstream components include the small GTPases Rho and Rac and activation of c-Jun N-terminal kinase (JNK), which act on components of the cytoskeleton, affecting change within a cell and in tissues (Okerlund et al., 2011). The Wnt/Calcium pathway also involves Wnt binding to a Frizzled receptor and activation via Disheveled. This results in an increase in cellular Calcium levels which then act on downstream effectors such as PKC CamKII (Mulligan et al., 2012).

These various Wnt pathways form a signaling network that regulate multiple aspects of neurodevelopment including cell fate specification, cell proliferation, cell migration, and embryonic axis patterning. Disruption of constituent parts of this network through mutation can conceivably increase susceptibility to psychiatric and neurodevelopmental disorders.

Wnt Signaling and Psychiatric Disorders

There have been many studies implicating Wnt signaling in psychiatric illness (Okerlund et al., 2011). Playing a critical role throughout development of the nervous system, Wnt signaling is a likely source of susceptibility to neural and psychiatric dysfunction when not functioning properly. This can be due to mutations in constituent genes of the various pathways, whereby a disruption in one or several components can have deleterious effects on a small or large part of the signaling network. This can in turn have a wide range of consequences, from mild to severe dysfunction, and result in different disease states. Wnt signaling is involved not only in brain regionalization, but also in the regulation of dendrite, dendritic spine, and synapse development- attributes that have a minimal effect on overall brain structure but are hypothesized to be important to psychiatric disease etiology (Mulligan et al., 2012). Adding to this, GSK3 is one of the central components of the Wnt signaling pathways and is also a pharmacological target of Lithium used to treat bipolar disorder as well as major depressive disorder. Recently, with the advent of genome wide sequencing, a multitude of Wnt genes have been identified as risk factors in the etiology of psychiatric disorders- most notably Autism Spectrum Disorders (ASD), but also Schizophrenia (Sz) and Bipolar Disorder (BD).

Dixdc1 and Wnt Signaling

Dix domain containing-1 (Dixdc1) is a cytosolic scaffold protein originally identified as a positive regulator of the canonical Wnt/β-Catenin signal transduction pathway required for proper neural patterning in zebrafish (Shiomi et al., 2003). Dixdc1 has a motif also present in Disheveled and Axin (hence DIX domain), two protein families critically important to Wnt signaling. Subsequent studies have found Dixdc1 to be widely expressed during development of the mammalian brain, as well as in the adult brain, most notably in the hippocampus, cerebral cortex, olfactory bulbs, dorsal thalamus, and cerebellum (Shiomi et al., 2005). Dixdc1 also functions in β-Catenin-independent (non-canonical) Wnt signaling, through its regulation of c-Jun N-terminal Kinase (JNK) activity (Wong et al., 2004; Ikeuchi et al., 2009). Additionally, Dixdc1 has a role in the regulation of axon growth and binds elements of the cytoskeleton (Ikeuchi et al., 2009; Wang et al., 2006; Wu et al., 2009). Recently, it was discovered that Dixdc1 regulates the schizophrenia risk gene Disrupted in Schizophenia-1 (DISC1). Dixdc1 binds to DISC1 and thereby modulate its roles in Wnt/β-Catenin-dependent neuronal proliferation and Wnt/β-Catenin-independent neuron migration in the developing cortex (Singh et al., 2010). Based on these published expression data, biochemical examination of intracellular binding partners (including DISC1), and in vivo RNAi analysis in the cerebral cortex, we hypothesized that Dixdc1 participates in neural development and is therefore critical for proper brain function. However, a comprehensive study to elucidate neurodevelopmental and molecular mechanisms of Dixdc1 action was required. Additionally, the published evidence that Dixdc1 participates in neurogenesis, neuron

migration, and axon growth was based on over-expression and RNAi-models, and required replication using a genetic system.

Dixdc1 in Neurodevelopment

To investigate the role of Dixdc1 in neurodevelopment, a Dixdc1 knockout (KO) mouse was generated using gene-targeting technology (Kivimae et al., 2011). These mice are homozygous viable and do not have any gross neural abnormalities; however, our behavioral analysis reveals that Dixdc1 knockout mice exhibit correlates of anxiety and depression as well as sociability deficits in behavioral assays. We have also used this mouse to investigate how loss of Dixdc1 influences Wnt signaling, and examined the neurodevelopmental function of Dixdc1 at the cellular and molecular level. In cultured hippocampal pyramidal neurons from Dixdc1 KO mice, we found that there were developmental defects at the spine and synapse level. Neurons from mutant mice had normal dendritic arborization in a mixed (primarily CD-1) background, but had fewer spines along these dendrites and a greater percentage of immature spines (filopodia). This suggests separate mechanisms for Dixdc1's involvement in dendrite development, whereby it is required for proper quantities of spines along the dendrite, but not for elaboration of the dendrites themselves. Likewise, Dixdc1 is required for proper maturation of those dendritic spines, both phenotypes which could have an effect on synapse development and number, ultimately leading to the observed behavioral differences in Dixdc1 KO mice and to an increased susceptibility to psychiatric and other neurodevelopmental disorders. Notably, in a BL/6 mouse background, mutant mice did have a slight, significant decrease in dendrite arborization, indicating this phenotype is genetic background dependent. To elaborate, it is possible that loss of

5

Dixdc1 has a negligible effect on dendrite arbor development by itself, but in conjunction with other genetic abnormalities found in specific mouse strains has a stronger effect on this phenotype. This is not surprising as we also observed differences in behavioral phenotypes in mutant mice in a BL/6 background (Kivimae et al., 2011).

In addition to the dendritic spine deficiency, pyramidal neurons from the hippocampus also had a reduction in the number of excitatory (glutamatergic) synapses, but not in the number of inhibitory (GABAergic) synapses. This was observed by quantifying pre- and post-synaptic marker co-localization along primary dendrites (VGlut1 and PSD-95 for excitatory, VGAT and Gephyrin for inhibitory synapses). A deficit in excitatory synapses could be due to the reduction in spine number and spine maturation- dendritic spines being the primary location of excitatory synapses in pyramidal neurons. It could also be due more directly to effects on Wnt signaling (either β-catenin dependent or independent) and the direct regulation of synaptic development. As neuropsychiatric disorders can be due in part at least to defects in synaptic signaling, this phenotype could be a potential explanation for the behavioral changes seen in Dixdc1 mutant mice and increase susceptibility to developing a psychiatric disorder. Having a reduction in the number of excitatory synapses could also create an imbalance in excitatory versus inhibitory synaptic signaling- another potential cause of psychiatric pathogenesis. These observations were also replicated in intact tissue by examining cortical pyramidal neurons in the neocortex expressing GFP.

A Role for Dixdc1 in Psychiatric Illness

With these behavioral and neurodevelopmental phenotypes, it is plausible that Dixdc1 plays a role in susceptibility to psychiatric illness. We therefore sought additional evidence for this at the pharmacological and genetic levels. As Dixdc1 has previously been shown to positively regulate Wnt/β-catenin signaling, that is the pathway we first chose to examine. The canonical pathway functions in large part by inhibiting GSK3, so inhibition of GSK3 pharmacologically could potentially rescue the observed behavioral and neurodevelopmental phenotypes. Lithium is a compound used to treat psychiatry patients, most notably Bipolar Disorder, that inhibits GSK3, among other molecular targets. In addition, there are several commercially available selective small molecule inhibitors of GSK3 (GSK3i). When mutant mice were treated with Lithium or GSK3i, motivational and sociability behaviors were rescued. The same was also seen with neurodevelopmental phenotypes- spine number and maturation and excitatory synapse number were rescued.

In addition to pharmacological and neurodevelopmental evidence, we also looked for genetic support of Dixdc1's involvement in psychiatry. We examined several databases that included thousands of ASD, Bipolar, and schizophrenia patient and control samples and found an increased burden of single nucleotide variants (SNV) in the Dixdc1 genetic loci of patients. Functional testing of SNVs from ASD patients revealed abnormalities in their ability to activate Wnt/β-catenin signaling and to rescue neurodevelopmental phenotypes, with some SNVs actually having dominant-negative effects in control neurons. Taken together, these data demonstrate a plausible role for Dixdc1 in psychiatric disease etiology.

References

Kiecker, C. and Niehrs, C. (2001) A morphogen gradient of Wnt/beta-catenin signalling regulates anteroposterior neural patterning in Xenopus. Development 128:4189–4201

Kivimae, S., Martin, P.M., Kapfhamer, D., Ruan, Y., Heberlein, U., Rubenstein, J.L., and Cheyette, B.N. (2011). Abnormal behavior in mice mutant for the Disc1 binding partner, Dixdc1. Transl Psychiatry *1*, e43.

Logan, C.Y. and Nusse, R. (2004). The Wnt Signaling Pathway in Development and Disease. Annu. Rev. Cell Dev. Biol., *20,* 781-810.

Mulligan, K.A., and Cheyette, B.N. (2012). Wnt signaling in vertebrate neural development and function. J Neuroimmune Pharmacol *7*, 774-787.

Okerlund, N.D., Kivimae, S., Tong, C.K., Peng, I.F., Ullian, E.M., and Cheyette, B.N. (2010). Dact1 is a postsynaptic protein required for dendrite, spine, and excitatory synapse development in the mouse forebrain. J Neurosci *30*, 4362-4368.

Okerlund, N.D., and Cheyette, B.N. (2011): Synaptic Wnt signaling-a contributor to major psychiatric disorders? J Neurodev Disord 3(2),162-174.

Shiomi, K., Uchida, H., Keino-Masu, K., and Masu, M. (2003). Ccd1, a novel protein with a DIX domain, is a positive regulator in the Wnt signaling during zebrafish neural patterning. Curr Biol *13*, 73-77.

Shiomi, K., Kanemoto, M., Keino-Masu, K., Yoshida, S., Soma, K., and Masu, M. (2005). Identification and differential expression of multiple isoforms of mouse Coiled-coil-DIX1 (Ccd1), a positive regulator of Wnt signaling. Brain Res Mol Brain Res *135*, 169-180.

Wang, X., Zheng, L., Zeng, Z., Zhou, G., Chien, J., Qian, C., Vasmatzis, G., Shridhar, V., Chen, L., and Liu, W. (2006). DIXDC1 isoform, I-DIXDC1, is a novel filamentous actin-binding protein. Biochem Biophys Res Commun *347*, 22-30.

Wong, C.K., Luo, W., Deng, Y., Zou, H., Ye, Z., and Lin, S.C. (2004). The DIX domain protein coiled-coil-DIX1 inhibits c-Jun N-terminal kinase activation by Axin and dishevelled through distinct mechanisms. J Biol Chem *279*, 39366-39373.

Wu, Y., et al. (2009). DIXDC1 co-localizes and interacts with gamma-tubulin in HEK293 cells. Cell Biol. International, 33, 697-701.

Chapter 2

DIXDC1 contributes to psychiatric susceptibility by regulating dendritic spine and glutamatergic synapse development via Wnt/β-catenin signaling

Summary

The scaffolding protein DIX domain containing 1 (DIXDC1) was first discovered as a positive regulator of Wnt/Beta-catenin signaling in zebrafish (Shiomi et al., 2003). Successive studies have implicated Dixdc1 as having a role in neurodevelopment, including axon elongation, neuronal migration, and neuronal proliferation (Ikeuchi et al., 2009; Singh et al., 2010). A link with psychiatric susceptibility was suggested in a study that found DIXDC1 interacts with Disc1, a gene found to have a strong correlation with various psychiatric diseases (Singh et al., 2010). This discovery, along with Dixdc1's involvement in Wnt signaling, led our group to investigate the role it has in neuronal development and behavior in a knockout mouse model of the gene. Previous studies utilized RNA knockdown- which can be problematic due to off target effects- to study the function of Dixdc1 in several aspects of neural development and signaling. Using a genetic approach, we hoped to gain a clearer picture for the role of DIXDC1 in these facets. Mice lacking DIXDC1, an intracellular Wnt pathway transducer upstream of Glycogen Synthase Kinase-3 (GSK3), have abnormal measures of anxiety, depression and social behavior. Pyramidal neurons in these animals' brains have reduced dendritic spines, mature spines, and glutamatergic synapses, and treatment with lithium or a specific GSK3 inhibitor corrects these phenotypes. Analysis of DIXDC1 in over 9,000 individuals with autism, bipolar disorder and schizophrenia reveals higher rates of rare inherited sequence-disruptive single nucleotide variants (SNVs) compared to controls.

Many of these SNVs disrupt Wnt signaling activity of the late neurodevelopmental DIXDC1 isoform; a subset that hyperactivate this pathway cause dominant neurodevelopmental effects. This demonstrates that DIXDC1 SNVs contribute to psychiatric pathogenesis by disrupting spine and glutamatergic synapse development, and supports that a major therapeutic action of lithium is to stabilize glutamatergic synapses via GSK3 inhibition. This project was a collaborative effort between members of the Cheyette lab and various other labs at UCSF and other institutions.

Introduction

Recent advances in human genomics are revolutionizing our knowledge of molecules conferring susceptibility to psychiatric disorders, but have also highlighted the complexity of genetic contributions to behavior and underscored the need to define common biological pathways contributing to psychiatric pathogenesis (De Rubeis et al., 2014; Krumm et al., 2014; Pinto et al., 2014).

One pathway proposed to play a role in psychiatric illness is Wnt/β-catenin signaling, a biochemical cascade conserved in all metazoans by which nearby cells communicate during and after development. This pathway plays critical roles throughout the organism during development and in a wide range of disease states. During central nervous system development it participates in, among other roles, brain regionalization, neural precursor proliferation, neural fate specification and synapse formation (Mulligan and Cheyette, 2012).

Evidence that the Wnt/β-catenin pathway contributes to the etiology and therapeutics of psychiatric illness comes from an array of sources: Pharmacologically,

several psychotogenic and psychotherapeutic drugs alter activity of the central Wnt/β-catenin pathway kinase, Glycogen Synthase Kinase 3 (GSK3) (Alimohamad et al., 2005; Hedgepeth et al., 1997; Svenningsson et al., 2003). In animal models, disruption of some Wnt/β-catenin pathway components leads to behavioral phenotypes reminiscent of human psychopathology (Kivimae et al., 2011; Long et al., 2004; Mohn et al., 2014). Human genetic studies support that variation at pathway loci contributes to the genetics of Autism Spectrum Disorder (ASD) (De Rubeis et al., 2014; Krumm et al., 2014; Martin et al., 2013; O'Roak et al., 2012; Pinto et al., 2014; Sanders et al., 2012; Zhou et al., 2007), including that *Chromodomain Helicase DNA binding 8* (*CHD8*), encoding a protein that co-regulates many Wnt/β-catenin transcriptional targets, has the highest genome-wide prevalence of *de novo* loss-of-function mutations in ASD (Iossifov et al., 2014).

DIX Domain Containing 1 (DIXDC1), a positive cytoplasmic transducer of the Wnt/β-catenin pathway (Shiomi et al., 2005; Shiomi et al., 2003), is of additional interest because it also interacts with Disrupted in Schizophrenia 1 (DISC1), a gene variously implicated in the genetics of psychiatric disorders including schizophrenia (Scz), major depression, bipolar disorder (BD) and ASD (Porteous et al., 2011; Singh et al., 2010). Moreover, compared to some core Wnt/β-catenin pathway components, DIXDC1 has a relatively restricted tissue distribution including in the late developmental and postnatal central nervous system (Shiomi et al., 2005; Soma et al., 2006). This suggests that DIXDC1 might have specialized roles in developing and mature neurons, and that functional *DIXDC1* variants might manifest in the human population as behavioral syndromes, as opposed to birth defects or non-neural diseases.

Here we describe a multifaceted analysis of DIXDC1 function in neural development and psychiatric pathogenesis. Using behavioral, neurodevelopmental, biochemical, and pharmacological analyses of a knock-out mouse model combined with human genetic analyses across several psychiatric disorders and functional analyses of rare missense mutations found in one set of such patients (ASD), we show that DIXDC1 participates in the regulation of dendritic spine and excitatory (glutamatergic) synapse formation downstream of Wnt/β-catenin signaling and upstream of behavior, particularly depression- and anxiety-like behaviors potentially relevant to affective disorders, and reciprocal social interactions potentially relevant to ASD.

Results

Depression, Anxiety, and Social Behavioral Abnormalities in *Dixdc1KO* Mice

We showed previously (Kivimae et al., 2011) that homozygous *Dixdc1* knock-out (*Dixdc1KO*) mice in an inbred C57Bl/6 (isogenic) background spend significantly less time in the open arms of a plus maze, a measure of anxiety, as well as increased total time immobile in the Forced Swim Test (FST), an assay for behavioral despair often regarded as a rodent model for depression (Cryan et al., 2005). However, *Dixdc1KO* mice in this genetic background also display reduced general activity; a confound for behavioral assays that rely on differences in activity as an output measure. Neurodevelopmental and behavioral phenotypes in inbred laboratory mice can be sensitive to isogenic background and this has occasionally confounded interpretation of other mouse models (Chadman et al., 2008; Koike et al., 2006; Long et al., 2004). Accordingly, we reprobed *Dixdc1KO* mice for behavioral and neurodevelopmental phenotypes that were sufficiently robust to remain significant even in an outbred (*CD-1*) genetic background, and used this background for all phenotypic characterization in this study.

Outbred *Dixdc1KO* mice are no different from wild type (WT*)* littermates in general activity or several other behavioral measures (Table S1), yet have a significantly decreased latency to immobility (Fig 1A, *left*) and spend significantly more total time immobile in the FST (Fig 1A, *right*). These mice also show a trend toward increased total time immobile in the tail suspension test, an independent assay for behavioral despair (Fig S1). Consistent with prior findings indicating an increase in some indicators of anxiety (Kivimae et al., 2011), homozygous *Dixdc1KO* mice spent significantly less time than WT littermates in the center versus surround of an open field (Fig 1B). Furthermore, in the

hyponeophagia assay which measures the balance between the drive to eat versus anxiety associated with approaching and sampling an unfamiliar food source (Deacon, 2011), *Dixdc1KO* mice show an increased latency to begin eating (Fig 1C. *left*) and decreased total time eating (Fig 1C, *right*).

Given previously established functions for Dixdc1 in Wnt/β-catenin signaling (Shiomi et al., 2005; Shiomi et al., 2003; Tan et al., 2015) and recent human genetic evidence suggesting that alterations in Wnt/β-catenin signaling contribute to ASD pathogenesis (Iossifov et al., 2014; Krumm et al., 2014), we asked whether *Dixdc1KO* mice have abnormalities in assays thought to model core symptoms of ASD – *i.e.* in social and repetitive behaviors. In fact, *Dixdc1KO* mice showed no differences in multiple assays for repetitive behavior, including the marble burying task, or frequency of spontaneous grooming, rearing, or digging (Table S1) (Deacon, 2006). They also showed no difference in the accelerating rotarod test, advanced as a potentially relevant motor test in some ASD mouse models (Rothwell et al., 2014), nor in other assays for motor behavior (Table S1). In assays of social behavior, *Dixdc1KO* mice showed no difference in the three chamber test, which measures the tendency to spend more time in a chamber with another animal confined within a smaller wire cage versus in a separate chamber where no such animal is present (Table S1) (Jamain et al., 2008). However, in the social interactions in pairs test (SIP), where 2 males of the same genotype freely interact within a closed arena (Jamain et al., 2008), *Dixdc1KO* mice spent significantly less time together than did *WT* littermates (Fig 1D, *left*). Interestingly, the decrease in total interaction time between *Dixdc1KO* animals in the SIP was not attributable to reduced total number or frequency of mouse-mouse interactions. Instead the difference on this assay was due to

a significant decrease in the average time *Dixdc1KO* mice spent during each interaction (Fig 1D, *middle*). Moreover, the longest single interaction was significantly shorter for *Dixdc1KO* mouse pairs compared to control pairs (Fig 1D, *right*). Interactions of longer duration in this assay were characterized by reciprocal social behaviors including nose-to-nose sniffing, nose-to-anogenital sniffing, or one animal following close behind the other, compared to interactions of shorter duration which often did not incorporate these components. The data therefore suggest that *Dixdc1KO* mice have a selective deficit in the social behavioral domain, specifically a deficit in reciprocal social interactions.

Pyramidal Neurons in *Dixdc1KO* Mice have Reduced Spines and Glutamatergic Synapses

Dixdc1KO mice are viable and fertile and have grossly normal brains with typical regional architecture (Kivimae et al., 2011) (Fig S2). We therefore searched for other neuronal phenotypes that might underlie behavioral differences in these animals. Studies of other neurodevelopmentally expressed Wnt pathway components and DISC1 have supported roles in dendrite, dendritic spine and glutamatergic synapse formation (Arguello et al., 2013; Hall et al., 2000; Hayashi-Takagi et al., 2010; Kerr et al., 2014; Okerlund et al., 2010). To initially probe for these phenotypes in the *Dixdc1KO* mouse line, we employed cultured hippocampal neurons because of their well-established validity as a model system for these neurodevelopmental processes in intact forebrain (Okerlund et al., 2010). Using this system, we found that neurons from *Dixdc1KO* neonates had normal dendrite arborization as assessed by Sholl analysis (Fig S3A-C) but compared to WT had significantly reduced dendritic spine density (Fig 1E, F) and a greater percentage of

immature (filopodial) spines (Fig 1E, G) along primary dendrites. We next confirmed that spine phenotypes identified in hippocampal neuron culture are present in pyramidal neurons within the cortices of these animals. To facilitate visualization of individual pyramidal neuron dendrites in brain tissue we crossed transgenic Thy1 fluorescent marker alleles (Thy1-GFP/YFP) that sparsely label deep layer (L5/6) cortical pyramidal neurons into the *Dixdc1KO* background (Feng et al., 2000). We collected cortical tissue from Thy1-GFP+ *Dixdc1KO* and *WT* littermates and quantified density and maturity of spines along apical dendrites of individual GFP-expressing pyramidal neurons (Arguello et al., 2013). Consistent with culture data, we found that pyramidal neurons within the cortices of *Dixdc1KO* mice had reduced dendritic spine density (Fig 1H, I) and a greater percentage of immature spines (Fig 1H, J).

Having observed similar spine deficits in both cultured neurons and fixed brain tissue we wished to measure spines dynamically in live animals, and so we imaged apical dendrites and spines in the somatosensory cortex of living Thy1-YFP+ mice using transcranial two-photon imaging. Here again we found that spine density on L5 apical dendrites was significantly reduced in *Dixdc1KO* compared to WT littermates at one month of age (Fig 1K, L). Interestingly, spine dynamics (proportion of spines formed and eliminated over 7 days) were not significantly different between *Dixdc1KO* and WT littermates at this stage (Fig 1M). These data support a developmental defect in spine formation in *Dixdc1KO* cortical pyramidal neurons that persists into early adulthood.

To functionally substantiate imaging findings, we conducted internal electrophysiological recordings from L5/6 corticothalamic pyramidal neurons in the prefrontal cortex. In *Dixdc1KO* mice these neurons had significantly reduced

hyperpolarization-activated cationic current (h-current; I_h) compared to WT littermates (Fig 1N, O) based on reductions in the voltage "sag" and rebound after hyperpolarization following a hyperpolarizing current pulse. This is consistent with reductions in the density of mature spines, the subneuronal sites where hyperpolarization-activated cyclic nucleotide-gated (HCN) channels reside (Paspalas et al., 2013). To corroborate this interpretation, we returned to fluorescent immunohistochemistry in Thy1-GFP[+] mice, using anti-HCN antibody to visualize channel puncta along dendrites of individual GFP-expressing L5/L6 pyramidal neurons. This confirmed a reduction in density of HCN puncta along dendrites of *Dixdc1KO* cortical pyramidal neurons (Fig 1P, Q).

Spines also correspond to the postsynaptic compartment of most glutamatergic inputs to pyramidal neuron dendrites (Paspalas et al., 2013). We therefore asked whether spine deficits in *Dixdc1KO* pyramidal neurons were accompanied by deficits in glutamatergic synapse density. Cultured hippocampal neurons from *Dixdc1KO* neonates had significantly reduced glutamatergic synapse density along dendrites as assessed by fluorescent confocal co-localization of specific pre- and post-synaptic molecular markers (Fig 1R, S). As with spine phenotypes, we confirmed this phenotype within cortical tissue of *Dixdc1KO* mice, observing a significant decrease in glutamatergic synapse density along apical dendrites of individual GFP-expressing pyramidal neurons (Fig 1T, U). In contrast to reduced glutamatergic synapse density, using similar methodologies we detected no difference in inhibitory (GABAergic) synapse density along dendrites of *Dixdc1K*O cultured hippocampal neurons, or along dendrites of pyramidal neurons within the cortices of *Dixdc1K*O mice (Fig S3D-G).

Neurons from *Dixdc1KO* Mice have Impaired Wnt/β-catenin Signal Transduction

The Wnt/β-catenin signal pathway is so named because the secreted glycoprotein ligand (any one of over a dozen related *WNT* proteins in mice and humans) binds to a transmembrane receptor complex on target cells, triggering a biochemical cascade that stabilizes free (non-membrane associated) β-catenin protein, which then acts as a transcriptional co-activator to alter gene transcription. Key intermediate proteins in the cytoplasmic signal transduction cascade include both Dishevelled (Dvl) and Axin plus several associated proteins. The centrally regulated enzyme downstream of Dvl and Axin is GSK3, which can phosphorylate β-catenin at serine 33 (S33), targeting it for degradation. It is this phosphorylation step that is regulated by the Wnt/β-catenin pathway.

The *Dixdc1* gene encodes multiple alternatively spliced isoforms; all transcripts share a common C-terminal region but isoform 1 (*aka* "A" or "long") encodes an additional N-terminal 211 amino acids including an actin-binding calponin homology domain not included in the other major transcript type, isoform 2 (*aka* "B") (Shiomi et al., 2005; Wang et al., 2006). We tested the ability of both isoforms to activate Wnt/β-catenin signaling in a standard cell-based assay (Biechele and Moon, 2008), confirming previous findings that isoform 2 but not isoform 1 robustly activates this pathway (Shiomi et al., 2005) (Fig 4D). These data combined with previous work suggests that the two main Dixdc1 isoforms have distinct primary cell biological functions: isoform 1 in signaling events upstream of cytoskeletal dynamics (Goodwin et al., 2014; Wang et al., 2006) and isoform 2 in Wnt/β-catenin signaling regulating gene expression (Shiomi et al., 2005; Shiomi et al., 2003). Because isoform 2 is the major late developmental and postnatal neural *DIXDC1* isoform

(Shiomi et al., 2005; Zhang et al., 2014) and is thereby likely to be relevant to psychopathology, we focused our studies on this isoform and the Wnt/β-catenin pathway, while another research group independently focused on functions of the *DIXDC1* gene in other signaling events during neural development (Kwan et al., 2016).

Given that Dixdc1 has a DIX domain that directly interacts with similar domains in the core cytoplasmic Wnt/β-catenin pathway components Dvl and Axin (Liu et al., 2011; Luo et al., 2005; Shiomi et al., 2005; Shiomi et al., 2003), we hypothesized that Wnt/β-catenin signal transduction would be impaired at the level of Dvl and Axin in differentiating pyramidal neurons of *Dixdc1KO* mice. We tested this hypothesis via several complementary approaches: First we tested whether Wnt/β-catenin signal pathway activity was altered in developing neurons of *Dixdc1KO* mice by directly measuring levels of β-catenin specifically unphosphorylated at the Wnt-pathway regulated residue S33 ("active β-catenin"). There was no difference in levels of active β-catenin in unstimulated *Dixdc1KO* versus WT cultured forebrain neurons (Fig 2A, B). However, treatment of these neurons with Wnt3a, an extracellular activator of this pathway (Moon et al., 1997), resulted in markedly different responses in *Dixdc1KO* versus WT. In WT neurons the level of active β-catenin rose markedly in response to Wnt3a, indicating the presence of intact Wnt/β-catenin signal transduction (Fig 2A, C). Contrastingly, in *Dixdc1KO* neurons there was no effect of Wnt3a treatment on active β-catenin level (Fig 2A, C). Because GSK3 is independently regulated by the AKT pathway, we asked whether markers for this pathway were also altered in *Dixdc1KO* versus WT neurons. In contrast to deficiencies observed in Wnt/β-catenin signal transduction, there were no differences in biochemical markers for the AKT pathway, including levels of phosphorylated AKT (p-AKT(Ser473))

19

or its specifically phosphorylated targets GSK3 (p-GSK3α(Ser21) and p-GSK3β(Ser9))

and β-catenin (p-β-cat(Ser522)) in *Dixdc1KO* neurons (Fig 2D).

The most universal transcriptional targets of the Wnt/β-catenin pathway are *Axin2* and

its molecular relative *Axin1,* encoding core Wnt pathway components that facilitate

physical interaction between GSK3 and β-catenin leading to β-catenin phosphorylation

and degradation; their transcription is activated in signal-receiving cells as part of a highly-

conserved negative feedback loop. We used these targets to confirm Wnt/β-catenin

signal pathway disruption in *Dixdc1KO* neurons through an independent methodology;

directly measuring levels of these transcripts by quantitative reverse-transcriptase

polymerase chain reaction (Q-PCR). There was no difference in mRNA levels of *Axin1*,

Axin2, or the control transcript *GAPDH* in unstimulated *Dixdc1KO* versus WT cultured

forebrain neurons (Fig 2E-G). This shows that in the absence of a Wnt signal, these

Wnt/β-catenin pathway target genes are transcribed at normal basal levels in *Dixdc1KO*

neurons. As expected, recombinant expression of a point-mutant-stabilized form of β-

catenin (β-cat(S33Y)) that bypasses the Wnt signal transduction pathway significantly

activated transcription of *Axin1* and *Axin2* in both *Dixdc1KO* and WT neurons while having

no effect on the control GAPDH transcript (Fig 2E-G). This demonstrates that Wnt target

genes can be activated in the *Dixdc1KO* mutant neurons if β-catenin is stabilized and can

enter the nucleus. However, treatment of neurons with Wnt3a results in markedly different

responses in *Dixdc1KO* versus WT neurons. In WT neurons levels of both *Axin1* and

*Axin*2 transcripts rise markedly in response to Wnt3a application, indicating intact Wnt/β-

catenin signal transduction in these cells. Contrastingly, in *Dixdc1KO* neurons this effect

of Wnt3a is greatly attenuated (Fig 2E, F). In combination, these data are fully consistent

with previous work identifying Dixdc1 as a protein that potentiates the Wnt/β-catenin signaling pathway at the level of Dvl: downstream of the transmembrane receptor complex and upstream of GSK3 and β-catenin; it further establishes that Dixdc1 is a significant contributor to Wnt/β-catenin signal pathway transduction in developing forebrain neurons.

In order to determine whether dendritic spine and glutamatergic synapse phenotypes arise from decreased Wnt/β-catenin signaling efficiency in *Dixdc1KO* pyramidal neurons, we sought to rescue neurodevelopmental phenotypes in these cells by stimulating the pathway upstream and downstream of the putative pathway block. As anticipated, treatment with the upstream ligand Wnt3a had no or minimal effect on spine and glutamatergic synapse phenotypes in *Dixdc1KO* cultured hippocampal neurons, whereas transfection with β-cat(S33Y), which bypasses the pathway to directly activate target genes in the nucleus, rescued spine and glutamatergic synapse phenotypes in these cells (Fig 2H-J). Interestingly, recombinant expression of β-cat(S33Y) in WT cultured hippocampal neurons significantly decreased spine and synapse density (Fig 2H, J), with little effect on immature spine percentage (Fig 2I). This suggests that either hypo- or hyper-stimulation of the Wnt/β-catenin pathway can lead to similar spine and synapse density reductions in pyramidal neurons.

Behavioral Phenotypes are Rescued by Lithium or a GSK3 Inhibitor

Supporting a strong genotype-phenotype correlation between the *Dixdc1KO* allele and behavioral phenotypes in the *Dixdc1KO* mouse line, we noticed that behavioral differences on the FST, the hyponeophagia assay, and the SIP were gene-dose sensitive,

with heterozygous *Dixdc1KO* mice displaying an intermediate phenotype (Fig 1A, C, D). We hypothesized that this reflects Dixdc1-dose-sensitive reductions in Wnt/β-catenin signaling activity in these animals. To test this hypothesis, we asked whether behavioral phenotypes in these animals could be corrected by treatment with the mood stabilizing agent lithium chloride, which among other cell biological effects activates the Wnt/β-catenin pathway through direct inhibition of GSK3 (O'Brien and Klein, 2009). Indeed, systemic injection of either lithium chloride or a selective small molecule GSK3 inhibitor (GSK3i) corrected behavioral phenotypes in *Dixdc1KO* animals, including in the FST (Fig 3A) and SIP (Fig 3B). Combined with reversible pharmacology (Fig S4), these data strongly support that these behavioral phenotypes in heterozygous and homozygous *Dixdc1KO* mice occur secondary to Dixdc1 gene-dose sensitive changes in the regulation of GSK3, specifically increased GSK3 activity.

Spine and Synapse Phenotypes are also Rescued by Lithium or a GSK3i

We hypothesized that the FST and social behavioral abnormalities in *Dixdc1KO* mice that are rescued by lithium and GSK3i correspond to an underlying GSK3-sensitive neuronal phenotype, and further that this underlying phenotype is the spine and glutamatergic synapse deficit observed in *Dixdc1KO* pyramidal neurons. We tested this hypothesis in animals treated with lithium chloride or GSK3i using an administration protocol identical to that which rescued behavioral phenotypes, assessing instead for effects on these neurodevelopmental phenotypes. Confirming our hypothesis, we found that systemic injection of either lithium or GSK3i rescued dendritic spine density, spine morphology, and glutamatergic synapse density in L5/6 pyramidal neurons within these animals' brains

22

(Fig 3C-K).

Inherited Rare Missense SNVs in *DIXDC1* Contribute to Psychiatric Susceptibility

Behavioral phenotypes and pharmacological responses in the *Dixdc1KO* mouse line described here suggest relevance of this model to psychiatric syndromes affecting social behavior, mood, and anxiety, while rare mutations in the Dixdc1 binding partner *DISC1* have previously been implicated in a variety of psychiatric conditions prominently including affective and psychotic disorders (Porteous et al., 2011). We therefore asked whether sequence variation at the *DIXDC1* locus might contribute to a corresponding range of psychiatric disorders. We first analyzed two datasets of exome sequences (Fig S5), totaling nearly 6000 ASD cases and over 7000 controls, focusing on SNVs most likely to affect Dixdc1 function: *i.e.* nonsense, missense and conserved splice-donor/acceptor-disrupting SNVs. This revealed a significantly greater burden of rare sequence-disrupting SNVs in the coding sequence for *DIXDC1* in ASD versus unaffected controls. This was true whether focusing on exons encoding isoform 1 (Fig 4B) or isoform 2 (Fig 4C), though the signal was more significant when restricting analysis to isoform 2 (Fig 4B*,* C and Fig S5A*,* B).

Next, we analyzed a sample of approximately 1000 BD patients and a similarly sized ethnically-matched control cohort. There was once again a greater burden of rare sequence-disruptive SNVs in both isoforms in BD cases versus controls (Fig 4B, C), though in this smaller sample set the signal reached significance only for isoform 1. Finally, we analyzed a dataset of over 2500 exome sequences from Scz patients and a similar number of ethnically-matched controls (Purcell et al., 2014). Here again, a greater

burden of rare sequence-disruptive SNVs in both isoforms was evident in patients versus unaffected controls, reaching significance for isoform 2 (Fig 4B, C).

In each psychiatric dataset (2 separate ASD datasets, 1 BD dataset, and 1 Scz dataset) there was an increased burden of rare sequence-disrupting SNVs in both DIXDC1 isoforms in patients compared to unaffected controls (Fig 4B, C and Fig S5A, B). Combining these datasets - totaling over 9000 cases and over 11000 controls - the collective increased burden of rare sequence-disruptive SNVs across psychiatric disorders was significant for each isoform (isoform 1, $p=1.7x10^{-3}$; isoform 2, $p=2x10^{-4}$; Fig 4B, C, Tables S2, S3).

Rare Missense SNVs from Psychiatric Patients Alter Wnt/β-catenin Signaling

Given our data demonstrating disrupted Wnt/β-catenin signal transduction in developing *Dixdc1KO* pyramidal neurons (Fig 2), plus our own (Fig 4D) and previous (Shiomi et al., 2005) findings showing selective function for isoform 2 versus 1 in this pathway, we tested rare missense variants discovered in our initial sequencing dataset (AASC, Fig S5B) for functional effects on Wnt/β-catenin signal pathway activation by isoform 2 using a standard cell-based assay (Biechele and Moon, 2008). We used site-directed mutagenesis to engineer each variant into a human DIXDC1 isoform 2 cDNA and tested them alongside the WT cDNA for effects on Wnt/β-catenin signaling. We found that most missense SNVs either consistently reduced or consistently increased activity of the encoded protein in Wnt/β-catenin signaling (Fig 4E).

Rare Missense SNVs from Psychiatric Patients Fail to Rescue Spine and Synapse

Deficits

To test for conservation of function between the mouse and human DIXDC1 proteins, we asked whether WT human DIXDC1 could rescue neurodevelopmental phenotypes when expressed in *Dixdc1KO* cultured hippocampal neurons. WT DIXDC1 isoform 2 was recombinantly expressed starting at 12 days in vitro (DIV12) and neurodevelopmental phenotypes assessed 6 days later (DIV18). We found that the WT human protein completely rescued spine density, spine maturity and glutamatergic synapse density in *Dixdc1KO* neurons (Fig 5A-C, white *vs.* black bars).

Given these rescue data, combined with our discovery that patients with ASD, BD and Scz carry a greater burden of rare missense SNVs and that many of these alter Wnt/β-catenin signaling activity of the encoded protein, we hypothesized that these SNVs might contribute to psychiatric pathogenesis by altering Wnt/β-catenin signal transduction upstream of spine and glutamatergic synapse development. To test this hypothesis, we assessed cDNAs containing these SNVs for their ability to rescue neurodevelopmental phenotypes in *Dixdc1KO* cultured hippocampal neurons. DIXDC1 isoform 2 cDNAs containing control-derived hypoactivating SNVs (K89I, C389F) partially rescued neurodevelopmental phenotypes (Fig 5A-C, blue bars *vs.* black). More remarkably, no cDNAs containing SNVs found in ASD rescued neurodevelopmental phenotypes (Fig 5A-C, purple and red bars *vs.* black).

Wnt/β-catenin Pathway Hyperactivating SNVs Cause Dominant Spine and Synapse Deficits

With allele frequencies ≤0.1%, each of these *DIXDC1* SNVs is present in a single

copy; to contribute to psychiatric pathogenesis they must therefore have a dose-dependent or dominant effect over the WT allele. To test for this, we assessed whether DIXDC1 cDNAs containing SNVs caused dominant neurodevelopmental effects when recombinantly expressed in WT cultured hippocampal neurons. The WT human DIXDC1 isoform 2 protein had no effect on spine density, spine maturity or glutamatergic synapse density when recombinantly expressed in WT neurons (Fig 5D-F, white *vs.* black bar). cSimilarly, no isoform 2 cDNAs encoding Wnt/β-catenin pathway hypoactivating SNVs, whether found in our control samples (K89I, C389F), our ASD samples (R154T, R249Q), or both (T401M), had dominant effects on neurodevelopment in these assays (Fig 5D-F, bars 3, 4 (blue), 6, 7 (purple), 9, 12 (red) *vs.* black). In contrast, all of the strongly hyperactivating SNVs (A87T, Q169R, K188N, Q218H and R367W) had dominant neurodevelopmental effects - *i.e.* decreased spine density (Fig 5D), increased immature spine percentage (Fig 5E) and decreased glutamatergic synapse density (Fig 5F; bars 5 (purple), 8, 10, 11, 13 (red) *vs.* black).

DISCUSSION

Biochemical Mechanisms Upstream of Dendritic Spine and Synapse Development
We report here that the neurally-expressed intracellular protein Dixdc1 is a positive regulator of dendritic spine and glutamatergic synapse formation. Several lines of evidence support a role for disrupted Wnt/β-catenin signaling in generating neurodevelopmental and behavioral phenotypes in *Dixdc1KO* mice and in the neurodisruptive effects of rare *DIXDC1* sequence variants found in human psychiatric

26

patients. First, we have shown that rare *DIXDC1* missense SNVs found in psychiatric patients interfere with the protein's Wnt/β-catenin signaling function *in vitro.* Second, we have shown that a subset of these SNVs that hyperactivate the Wnt/β-catenin pathway cause dominant neurodevelopmental effects on spine and synapse formation, whereas similar SNVs that do not hyperactivate the Wnt/β-catenin pathway do not cause dominant effects. Third, we have shown that Wnt/β-catenin signaling hypoactivity, as expected to occur as a result of heterozygosity for a loss-of-function SNVs at this locus, is associated with similar neurodevelopmental and gene-dose-sensitive behavioral phenotypes in a knock-out mouse model. Fourth, we have shown that pharmacologically mimicking Wnt/β-catenin pathway activation via direct inhibition of GSK3, whether by the psychiatric drug lithium chloride or a selective small molecule GSK3 inhibitor, corrects neurodevelopmental and behavioral phenotypes in the *Dixdc1KO* mouse model.

Taken together, these data present a compelling case that Dixdc1 contributes to formation of dendritic spines and glutamatergic synapses via facilitation of Wnt/β-catenin signal transduction within differentiating pyramidal neurons. Moreover, our data suggest that rare missense variants in *DIXDC1*, even when present in a single copy, can contribute to psychiatric susceptibility by decreasing or increasing Wnt/β-catenin signal transduction in developing pyramidal neurons, thereby disrupting formation of spines and glutamatergic synapses. This is consistent with evidence from large-scale sequencing and other studies showing that loss-of-function mutations in either Wnt/β-catenin pathway inhibitors (*e.g.* CHD8, APC) (Iossifov et al., 2014; Zhou et al., 2007) or activators (*e.g.* CTTNβ1, WNT1) (Krumm et al., 2014; Martin et al., 2013; O'Roak et al., 2012) contribute to susceptibility for ASD, and combined with other data presented here (Fig 2H, J),

supports prior suggestions that either hypo- or hyper-activation of this morphogenic pathway has similarly deleterious effects on neurodevelopmental processes relevant to psychiatric pathogenesis (Kalkman, 2012).

That said, we cannot rule out that additional mechanisms may contribute to these neurodevelopmental and behavioral outcomes. For example, a β-catenin-independent mechanism downstream of GSK3, such as one that acts directly on cytoskeletal proteins (Ciani et al., 2004), could also be important in mediating spine and synapse formation. Moreover Dixdc1 has been implicated in other signaling cascades including PI3K-AKT/AP-1 (Wang et al., 2009; Xu et al., 2014), CKD5-DISC1-Ndel1 (Singh et al., 2010), upstream of JNK (Ikeuchi et al., 2009; Wong et al., 2004), in direct binding to actin (Wang et al., 2006), and in a MARK1/MARK4-dependent pathway downstream of LKB1 (Goodwin et al., 2014). With regard to the latter and to work conducted in parallel to our own (Kwan et al., 2016), it is plausible that distinct DIXDC1 isoforms are active in at least two major pathways upstream of dendritic spine and glutamatergic synapse development: one via MARK1 and one via GSK3, affecting both cytoskeletal dynamics and gene expression. In fact an intriguing possibility is that individual missense *DIXDC1* SNVs affect these pathways via distinct transcripts with a synergistic outcome on neuronal differentiation; a notable example is SNV T401/612M, found 10 times in cases versus 3 in controls across psychiatric disorders in our study (Tables S2, S3), plus an additional 2 times in separate ASD cases in the companion study (Kwan et al., 2016). This SNV affects both the ability of isoform 2 to activate Wnt/β-catenin signaling (Fig 4C) and the ability of isoform 1 to be phosphorylated by MARK1 (Kwan et al., 2016). Ongoing research in both the Cheyette and Singh laboratories will shed light on how these

biochemical pathways interact via *DIXDC1* to regulate neural development and behavior relevant to psychiatric pathogenesis.

Lithium and GSK3 Inhibition Upstream of Glutamatergic Synapses

Recent genomic and pharmacological studies suggest that the pathophysiology of ASD, Scz, as well as of major affective and anxiety disorders overlaps, and that it involves formation, maintenance, removal and function of glutamatergic synapses (De Rubeis et al., 2014; Duman, 2014; Krumm et al., 2014; Musazzi et al., 2013; Pinto et al., 2014; Sekar et al., 2016). Our findings fit neatly into this narrative, adding further evidence that abnormal glutamatergic synapse development contributes to psychiatric symptomatology including core features of autism, depression, anxiety and psychosis.

Several different biochemical mechanisms have been proposed to underlie the anxiolytic, antidepressant and mood-stabilizing properties of lithium, a drug whose systematic use in modern psychiatry began in the first half of the last century (Shorter, 2009). Lithium's best-validated mechanisms of action are inhibitory effects on IMP and INPP1, central phosphatases in the phosphoinositide pathway, and on GSK3, the key regulated kinase in the Wnt/β-catenin and AKT pathways (Lenox and Wang, 2003). Our data showing that loss of Dixdc1 in mice leads to impaired neuronal Wnt/β-catenin signal transduction and to gene-dose-sensitive behavioral phenotypes rectified by treatment with either lithium or a selective GSK3 inhibitor, support the latter as a major contributor to lithium's clinically useful activity. Moreover, our finding that these effects correlate with spine and glutamatergic synapse phenotypes in forebrain neurons suggests that these subneuronal structures are critical biological substrates for lithium's therapeutic action.

This strongly supports emerging evidence (Higgins et al., 2015; Kondratiuk et al., 2016; Liu et al., 2013) that lithium's psychiatric utility is rooted in increasing the formation and stability of glutamatergic synapses via inhibition of GSK3 in neurons.

EXPERIMENTAL PROCEDURES

In vivo imaging of spine dynamics

Male and female YFP-positive mice aged P(28-32) were used for *in vivo* two photon imaging of apical dendrites of cortical layer 5 pyramidal neurons. The procedures for transcranial imaging and data quantification have been previously described (Xu et al., 2009). The percentage of eliminated and formed spines were calculated as the number of spines eliminated or formed between the day 0 and day 7 imaging sessions, divided by the number of spines counted in the day 0 imaging session. Spine densities were calculated from image stacks collected on the day 0 imaging session by dividing the number of spines by the length of the dendritic segment traced in ImageJ.

Human sequencing samples

ASD:

ARRA ASD Sequencing Collaboration (discovery dataset)

VCF files were obtained from the dbGAP entry for the ARRA ASD Sequencing Collaboration (phs000298). Sequencing calls made by both the Broad Institute (534 ASD patients and 379 ethnically-matched European controls) and Baylor College of Medicine (505 ASD patients and 491 ethnically-matched European controls) were analyzed.

ASC (replication dataset)

As described (Sanders et al., 2015).

BD

The BD dataset included exome sequence data on 1,135 cases and 1,142 ethnically matched controls. Cases were ascertained as part of the Chicago, Hopkins, NIMH Intramural Program (CHIP) Bipolar Disorder study (n=94), and the National Institute of Mental Health (NIMH) Genetics Initiative Bipolar Disorder Collaborative study waves 1-5 (n=1,041) (Nurnberger et al., 1997). Controls, which were obtained from the NIMH Genetics Initiative repository (https://nimhgenetics.org/), were originally recruited by Knowledge Networks, Inc. (Menlo Park, CA) from participants in a nationally representative marketing panel (Sanders et al., 2008). All participants provided IRB-approved, written informed consent. Samples were sequenced using NimbleGen SeqCap EZ Exome v1 and v2 capture arrays and paired-end sequencing with either an Illumina GA-IIx or HiSeq 2000. Reads were aligned and variants called with Genome Analysis Toolkit (GATK) (McKenna et al., 2010) using Unified Genotyper with all samples together. High quality data on bi-allelic SNVs were retained for analysis.

Scz

As described (Purcell et al., 2014).

Burden analysis

Analysis was limited to nonsense, missense, and ultraconserved splice donor/acceptor site-disrupting rare SNVs, defined as minor allele frequency <0.1% in ExAC (accessed 8/2015). Percentages of individuals in case *vs.* control groups harboring these SNVs was compared by one-tailed Fisher's exact or one-tailed Chi square test as appropriate.

Genetics

The Dixdc1KO mouse line is the product of gene-targeting that replaced several critical exons of the Dixdc1 locus with a neo interrupter cassette, resulting in loss of Dixdc1 gene products confirmed at the mRNA (Kivimae et al., 2011) and protein levels (Fig S1A). All animal studies were performed in this mouse line maintained in an outbred CD-1 genetic background (Charles River). All comparisons were made in cohorts of littermate mice, separated by genotype blind to experimenter. Tg(Thy1-EGFP)M and Tg(Thy1-YFP)H alleles (The Jackson Laboratory) were crossed into the Dixdc1KO line to produce lines for confocal immunohistology of neurons in fixed tissue, and for transcranial 2-photon imaging of spine dynamics in living animals, respectively.

Animals

All procedures involving animals were carried out in accordance with IACUC-approved animal use protocols and conditions established by the Administrative Panels on Laboratory Animal Care at the University of California, San Francisco (Cheyette/Sohal) and at the University of California, Santa Cruz (Zuo).

Drug treatments

Lithium Chloride: P90-120 mice were given a single I.P. injection of 400 mg/kg LiCl or saline in a volume of 4 ml/kg, 5 hours prior to either the commencement of the FST, SIP,

or perfusion for histology. Lithium: FST n=4-9 mice/group; SIP n=12 mice/group. Vehicle FST n=14 mice/group; SIP n=6-10 mice/group.

GSK3i: P90-120 mice were given a single I.P. injection of 10 mg/kg SB216763 or saline in a volume of 4 ml/kg 5 hours prior to either the commencement of the FST, SIP or perfusion for histology. SB216763: FST n=8-12 mice/group; SIP n=12-14 mice/group. Vehicle FST n=14 mice/group; SIP n=12 mice/group.

Behavioral Assays

Social interactions in pairs test (SIP) (n=30-34 mice/group)

As described (Jamain et al., 2008). The test was performed in a neutral cage (white Plexiglas box, L37 x W33 x H33 cm). One day prior to the test day, each individual mouse went through one 10 min session in the neutral cage to habituate to the testing conditions. On test day, pairs of unfamiliar mice with the same genotype were placed into the neutral cage for 10 min. The time spent in social interaction (defined as sniffing or chasing) was registered.

Open field (n=35-44 mice/group)

The test was performed in a neutral cage (white Plexiglas box, L37 x W33 x H33 cm). Total distance travelled (as a measure of spontaneous locomotor activity) and proportion of distance travelled in the center area (10x10 cm) of the cage (as a measure of anxiety) was measured using a digital camera and ANY-maze Video Tracking System software (Stoelting Co., Wood Dale, IL, USA).

Three-compartment chamber (n=8 mice/group)

As described (Jamain et al., 2008). The social testing arena was a rectangular, three-chambered box. Each chamber was 20 x 40 x 22 cm in size. Dividing walls were made from clear Plexiglas, with rectangular openings (4 cm x 5 cm) allowing access into each chamber. The chambers of the arena were cleaned between trials. The test mouse was first placed in the middle chamber and allowed to explore it for 10 min. The openings into the two side chambers were obstructed during this habituation phase. After the habituation period, an unfamiliar WT CD1 male mouse (stranger), which had no prior contact with the subject mouse, was placed in one of the side chambers. The location of the stranger mouse in the left vs. right side chamber was systematically alternated between trials. The stranger mouse was enclosed in a small (6 cm diameter x 10 cm H), round wire cage (Galaxy cup, Spectrum Diversified Designs, Inc, Streetsboro, OH), which allowed nose contact through the bars but prevented fighting. The animals serving as strangers had previously been habituated to placement in the small cage. An identical empty wire cage (object) was placed in the opposite chamber. A weighted cup was placed on the top of the small wire cages to prevent climbing by the test mice. Both openings to the side chambers were then unblocked and the subject mouse was allowed to explore the entire social test arena for a 10 min session. The amount of time spent in each chamber and the time spent sniffing the stranger mouse or the empty cage were recorded. An entry was defined as all four paws in one chamber. At the end of the first 10 min, each mouse was tested in a second 10 min session to quantify social preference for a new stranger. A second, unfamiliar mouse (stranger 2) was placed into the previously empty wire cage. The test mouse had a choice between the first, already-investigated mouse (familiar), and the novel unfamiliar mouse. As described above, measures were taken of

the amount of time spent in each chamber and the time spent sniffing each mouse during the second 10 min session.

Digging (n=8 mice/group)

As described (Deacon, 2006). Briefly, a clear plastic container (L20xW20xH20 cm) was filled 7.5 cm deep with wood chip bedding, lightly tamped down to make a flat, even surface. The bedding substrate was flattened and firmed down again between mice. Test duration was 5 min. The latency to start digging, the number of digging bouts and the total duration of digging was recorded. Digging was defined as coordinated movements of fore or hind limbs that displace the substrate.

Marble burying (n=12-13 mice/group)

As described (Deacon, 2006). Briefly a clear plastic housing cage (L32xW18xH14 cm) was filled 5 cm deep with wood chip bedding, lightly tamped down to make a flat, even surface. The bedding substrate was flattened and firmed down again between mice. Fifteen glass marbles were placed on the surface, evenly spaced, each about 4 cm apart and one animal was left in the cage for 30 min. At the end of the test the number of marbles buried (to 2/3 their depth) with bedding was counted.

Forced Swim Test (FST) (n=28-29 mice/group)

As described (Silverman et al., 2010). Swim sessions were conducted by placing mice in individual polycarbonate cylinders (46 cm tall and 21 cm in diameter) filled with water (28-30°C water) to a depth of 15 cm. The depth was such that mice could not support themselves by placing their paws on the base of the cylinder. A standard 6-min test duration was employed. The water was changed between subjects. Latency to immobility and duration of immobility were measured. A mouse was judged to be immobile when

making only those movements necessary to keep its head above water. The first immobility bout was defined as immobility lasting more than 3 sec and occurring after the first 10 sec, to avoid measuring random behavior in reaction to first water immersion.

Zero maze (n=8 mice/group)

The zero maze consists of a circular platform (6.1-cm width with a 40-cm inner diameter) that is equally divided into four quadrants. Two quadrants on opposite sides of the platform are enclosed by walls (7 cm high); the other two quadrants are open and bordered by a lip (0.6 cm high). The maze is elevated 50 cm above the floor. The mouse was placed inside a closed arm, with all four paws inside, and its nose pointing toward the open arm. Time, distance traveled and number of entry in the open and closed arms was recorded for 5 min. Proportion of time spent in closed arms was used as an estimation of open arm aversion.

Tail suspension (n=14-16 mice/group)

As described (Silverman et al., 2010). Briefly, using adhesive tape, animals were suspended by the tail from the edge of a table elevated 70 cm. When suspended, rodents either make "escape

attempt" movements, or adopt a characteristic immobile posture. The latency to first immobility and the total time for which the mouse was immobile were measured during a 6 min test period.

Tube Test (n=8 mice/group)

In the tube test, mice were placed into opposite ends of an acrylic cylindrical tube (3.5 cm diameter x 30 cm length), and the mouse that retreated backward was noted. The percentage of retreats was calculated from the total number of encounters. Each mouse

was tested against 1 mouse of the opposite genotype from a different cage. On the day prior to data collection, each mouse was allowed to walk through the tube one time.

Rotarod (n=12-14 mice/group)

As described (Rothwell et al., 2014). Briefly mice underwent 2 trials per day over the course of 3 days in either a 4-40 rpm or a 8-80 rpm accelerating rotarod. Each trial ended when a mouse fell off, made successive complete backward revolutions while hanging on, or reached 300s.

Y-Maze (n=6-8 mice/group)

The Y-Maze spontaneous alternation test is a behavioral test for measuring the willingness of rodents to explore new environments. The maze consists of a Y-shaped maze with three white, opaque plastic arms at a 120° angle from each other. After introduction to the center of the maze, the animal is allowed to freely explore the three arms for 5 min. Each choice is recorded, and the spontaneous alternation score is determined by dividing the number of three successive choices that include one instance of each arm by the total number of opportunities for alternation.

Hyponeophagia (n=20-23 mice/group)

Mice were rationed for food overnight for a single night. For this, we removed ad lib food from the cage hopper the evening before testing and replace it with 1 g/mouse of ordinary diet, which is approximately a third of what the animals would normally eat over the course of the night. When they were group housed we cut the chow pellets into small pieces to ensure that all the mice can eat equal shares. Mice were tested the next morning and resume an ad-lib feeding regimen as soon as testing is finished. Testing: A translucent plastic jug (approximate volume 1.5 l, 15 cm diameter with a spout protruding a further 2

cm) is placed upside down with the spout forming a small alcove over a small food well filled with full cream sweetened condensed milk (Nestle Carnation) diluted 50:50 with water as the novel food. The mouse is placed facing away from the well and the jug is gently lowered into position. Test duration is 6 min. Time eating in the first 2 min and latency to eat is recorded. Sniffs at the milk do not count; at least two sec of drinking must occur to be scored as a bout of ingestion.

Primary Neuronal Culture

As described previously (Okerlund et al., 2010). Briefly, hippocampi were dissected from neonatal (P0) mice, pups genotyped, and hippocampi of the same genotype pooled and cultured together starting the next day. Neurons were cultured for 18 days and fixed with 4% paraformaldehyde (PFA) in PBS. Neurons were transfected with pEGFP C1 (Clontech) at DIV14 for visualization of pyramidal neurons. Rescue experiments with Dixdc1 were performed as previously described but in addition to GFP, neurons were also transfected with either WT or a variant Dixdc1 cloned into p3XFLAG-CMV-10 (Sigma-Aldrich). For experiments examining the effect of Wnt/β-catenin pathway activation on neurodevelopment in culture, neurons were treated with the Wnt pathway activators as described below (Q-PCR).

Confocal imaging and analysis of spines and synapses (fixed tissue)

As described previously (Arguello et al., 2013; Okerlund et al., 2010). Briefly, fluorescence images were acquired on a Nikon Spinning Disk Confocal using a 40x or 60xoil objective. All images were analyzed using NIH ImageJ software. Synaptic puncta and dendritic spine quantification was performed on primary hippocampal cultures and were counted along GFP-labeled primary dendrites of an individual neuron from the soma to the first

branch point. Dendritic projections were binned on the basis of their morphology as filopodia or mature spines. 40-60 neurons total were analyzed for each genotype and each condition, collected from multiple different wells, and at least 9 animals per genotype. GFP$^+$ pyramidal neurons in the lower layers of the cortex were selected for synaptic puncta colocalization in P90 brain sections. Colocalization was scored if pre- and post-synaptic puncta along GFP-labeled primary dendrites overlapped by at least 1 pixel (i.e. 0.01 µm2). 30–50 neurons total were analyzed for each genotype, collected from at least 3 animals per genotype.

Wnt/β-catenin pathway luciferase reporter assay

As described previously (Biechele and Moon, 2008). Briefly, HEK293T cells were transfected with 1.6 □g pcDNA3.1(−) vector containing either the WT DIXDC1 cDNA, corresponding to the allele found on >99.8% of chromosomes in the Exome Aggregation Consortium database (ExAC; Cambridge, MA; http://exac.broadinstitute.org), or a cDNA containing an engineered mutation corresponding to an SNV. HEK293T cells were additionally transfected with 130 ng per well pBAR-Luc plasmid and 13 ng per well pRL-TK (Renilla luciferase control plasmid). Cells were cultured for 24 h, and then luciferase activity measured using the Dual-Luciferase Reporter Assay System (Promega, Madison, WI, USA) and an Envision multi-label plate reader (PerkinElmer, Waltham, MA, USA).

Quantitative reverse transcription-PCR (Q-PCR)

Cultured forebrain neurons were maintained for 18 days before lysis to extract RNA from cells. To express β-cat(S33Y), neurons were transfected with pcDNA3-(S33Y)β-catenin, a gift from Eric Fearon (Addgene plasmid # 19286) (Kolligs et al., 1999), at DIV14. To activate the Wnt/β-catenin pathway upstream, they were treated with 5nM Wnt3a (R&D

Systems) at DIV16. Media was changed on all cells during each treatment and twice per week otherwise. RNA lysis was done using the PureLink RNA mini kit (Ambion/Life Technologies) according to standard protocols. 1μg of RNA was used to perform the reverse transcription using the SuperScript VILO cDNA synthesis kit designed for QPCR (Life Technologies). QPCR was performed using the TaqMan QPCR system (Ambion) according to protocol provided with the kit. Analysis was done using the delta-delta-Ct method (Livak and Schmittgen, 2001) for relative gene expression using GAPDH as the normalizing gene.

Immunocytochemistry

Cultured forebrain neurons were fixed for 20 min in 4% PFA in PBS. After fixation cells were washed with PBS 3x for 5 min then blocked for 1 hour (blocking solution: 10% bovine serum albumin (BSA)+ 0.3% Triton X-100 in PBS) at room temperature. Neurons were incubated with primary antibodies overnight at 4ºC: mouse anti-HCN1 (1:200;Millipore), or rabbit anti-VGlut1 (1:500;Synaptic Systems) and mouse anti-PSD-95 (1:200;Neuromab) or rabbit anti-VGAT (1:200;Synaptic Systems) and mouse anti-Gephyrin (1:200;Synaptic Systems). After three 5 min washes in PBT (PBS with 0.3% Triton X-100), fluorescent secondary antibodies (1:400; Alexa 568 and Alexa 647 anti-rabbit or anti-mouse antibodies; Invitrogen) were applied in blocking solution for 1 hour at room temperature. After three 5 min washes with PBT, cells were washed with PBS and mounted in Mowiol mounting media (Thermo Fisher Scientific).

Brain Immunohistochemistry

Essentially as described (Arguello et al., 2013). Briefly, P90 mice were deeply anesthetized with Avertin (Sigma) and intracardially perfused with PBS followed by 4%

PFA. Brains were removed and post-fixed 4 hours in 4% PFA at 4ºC, followed by cryoprotection by immersion in 30% sucrose in PBS at 4ºC overnight. Brains were frozen in 2:1 30% sucrose: OCT (Tissue-Tek) on dry ice and stored at -80ºC. Brains were cut at 20 um on a Leica cryostat and mounted on Tissue Path Superfrost/Plus gold (Fisher Scientific) slides. Mounted brain sections were warmed with PBS for 5 min at room temperature followed by treatment with 3% Hydrogen Peroxide for 20 min at room temperature. Sections were then washed 3x 5 min with PBS and 2x 5 min with PBT. Sections were stained in a humid chamber with mouse anti-VGlut (1:200; Synaptic Systems) and rabbit anti-PSD-95 (1:200; Cell Signaling) or rabbit anti-VGAT (1:200;Synaptic Systems) and mouse anti-Gephyrin (1:200;Synaptic Systems) for 48 hours. Sections were washed 3x 5 min with PBT (PBS with .5% Triton X-100) then incubated with secondary antibody (1:400; Alexa 568 and Alexa 647 anti-rabbit or anti-mouse antibodies; Invitrogen) for 2 hours at room temperature. Sections were then washed 3x 5 min in PBT and 2x 5 min in PBS and cover-slipped with Mowiol.

In situ hybridization

As described (Fisher et al., 2006).

Nissl staining

P90-120 mouse brain cryosections were stained as follows: 15 min in 95% ethanol, 1 min in 70% EtOH, 1 min in 50% EtOH, 2 min in MQ H2O, 1 min in MQ H2O, 2 min in Cresyl Violet stain, 1 min in MQ H2O, 1 min in 50% EtOH, 4 dips in 70% EtOH +1% glacial acetic acid, 4 dips in 95% EtOH, 4 dips in 95% EtOH, 1 min in 100% EtOH and 5 min in 100% xylenes.

Immunoblotting

β-catenin/ P-GSK3/P-AKT

Western blots were performed on primary cortical neurons which were cultured for 18 days in vitro. Protein concentrations were normalized using BCA analysis (Thermo Scientific) and loading was confirmed via Ponceau S staining. All westerns were performed using 4-12% Bolt Bis-Tris gels (Life Technologies) with MOPS-SDS running buffer. Gels were run at 200 Volts for 25 min. Transfer to PVDF membrane was performed at 20V for 70 min. Incubation with active β-catenin (ABC) primary antibody (1:1250 dilution, Millipore), total β-catenin (1:1000 dilution, AbCam), P-β-catenin Ser552 (1:1000 dilution, Cell Signaling), P-GSK3α/β Ser21/9 (1:1000 dilution, Cell Signaling), P-AKT Ser473 (1:1000 dilution, Cell Signaling) and VDAC (1:1000 dilution, AbCam) was done overnight at 4°C. Incubation with secondary rabbit and mouse HRP-linked antibodies (1:2500 dilution, Cell Signaling) was done for one hour at room

temperature. Membranes were exposed using 1mL of ECL substrate (Cell Signaling) on standard film (Thermo Scientific). Quantification was performed using ImageJ software.

Dixdc1

The entire forebrains of P0 pups were sonicated in 1mL N-PER with phospho-stop and protease inhibitors per 100mg of tissue. Lysate was centrifuged, supernatant removed and the pellet was discarded. Resultant lysate was used for immunoprecipitation as follows: 25μl of primary antibody (Ccd1/Dixdc1; R&D Systems) was added to 1mL of brain lysate overnight at 4ºC. The antibody-lysate mixture was then incubated with 50μl of protein-G Dynabeads (Thermo-Fisher) for 45 min at 4ºC. The resulting sample was then run on a 4-12% bis-tris gel (NuPage-Bolt; Thermo-Fisher) and transferred to PVDF. The membrane was blocked for one hour at room temperature using 5% BSA and then

incubated with primary antibody (Ccd1/Dixdc1; R&D Systems) overnight at 4ºC. No-antibody controls were performed via the same protocol, except no antibody was added to the lysate prior to the addition of the protein-G beads.

Electrophysiology

Injection of retrogradely transported tracers

To selectively label medial prefrontal cortical corticothalamic neurons, we injected fluorescently-labeled cholera toxin subunit B (CTB, Lumafluor, Inc.; 400 nL at 100 nL/min) into ipsilateral mediodorsal thalamus using the following coordinates: -1.7 AP, +0.3 ML, and -3.5 DV. We waited 5 min after the end of the injection before slowly withdrawing the syringe. We waited 3-5 days following retrograde tracer injections before performing experiments, and we verified that retrograde tracer was not present in nearby structures such as striatum.

Slice electrophysiology

Animals of both sexes were used for all experiments. Mice 8-12 weeks old were deeply anesthetized with isoflurane and then decapitated. We prepared coronal slices 250 μm thick using ice-cold solution containing (in mM): 234 sucrose, 26 NaHCO3, 11 glucose, 2.5 KCl, 10 MgSO4, 1.25 NaH2PO4, and 0.5 CaCl2. ACSF contained (in mM): 126 NaCl, 26 NaHCO3, 14 glucose, 3 KCl, 2 CaCl2, 2 MgCl2, and 1 NaH2PO4. Slices were incubated in a warmed 50/50 mixture of ACSF and slicing solution at 30-32°C for 15 min and then at least one hour at room temperature before being used for recordings. During experiments, slices were perfused with ACSF and secured by placing a harp along the midline between the two hemispheres.

Intracellular recording

Somatic whole-cell patch recordings were obtained from visually identified neurons in L5/6 of infralimbic or prelimbic prefrontal cortex using differential contrast video microscopy on an upright microscope (BX51WI; Olympus). Recordings were made using a Multiclamp 700A (Molecular Devices). Patch electrodes (tip resistance = 2–6 MΩ) were filled with the following (in mM): 118 K-gluconate, 10 KCl, 10 HEPES, 4 MgATP, 1 EGTA, and 0.3 Na3GTP (pH adjusted to 7.2 with KOH). Slices were continuously perfused with ACSF in an immersion chamber (Warner Instruments) with temperature maintained at 32.5±1°C. Series resistance was usually 10–20 MΩ, and experiments were discontinued above 30 MΩ or if action potentials failed to overshoot 0 mV.

We did not correct for liquid junction potential. We measured resting membrane potential in current clamp immediately following whole cell break in. Input resistance was calculated from

the steady-state voltage change measured in response to -50 pA current steps. Action potential firing was quantified during current steps from -250 to +250 pA in 50 pA intervals. We calculated action potential frequency as the number of action potentials fired during the one-sec depolarizing current step 100 pA above rheobase. Amplitude of the hyperpolarization-activated cyclic nucleotide-gated (HCN)-mediated current was estimated in current clamp by summing the absolute values of the voltage sag and rebound depolarization in response to a -200 pA, 1 sec current pulse (Gee et al., 2012).

Statistical analysis

Unless stated otherwise in figure legends, the data are expressed as mean ± s.e.m. Data were analyzed by Student's *t*-test, 2-way ANOVA followed by multiple comparisons, Chi

square or Fisher's exact test using GraphPad Prism software (GraphPad Software, La

Jolla, CA, USA). A *P*-value of <0.05 was considered significant.

Figure 2.1

46
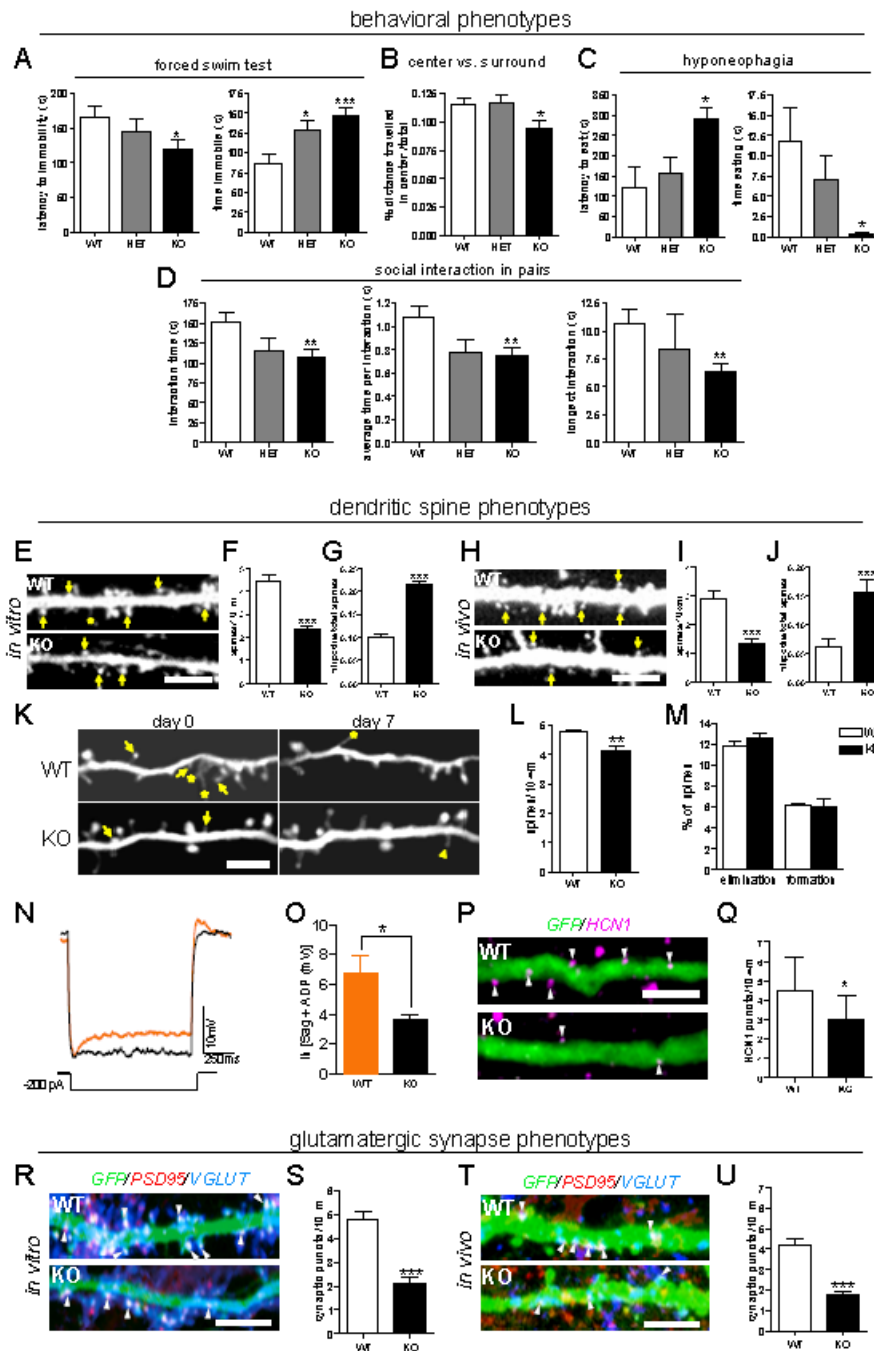
Figure 2.1. Behavioral and Neurodevelopmental Phenotypes in *Dixdc1KO* Mice

(A-D) Behavioral Phenotypes. **(A)** Behavioral despair (FST). *Dixdc1KO* mice start immobility bouts significantly sooner (*left*) and spend significantly more time immobile (*right*) than WT. **(B)** Anxiety (Open field) *Dixdc1KO* mice spend significantly less time in the center *vs.* surround of an open field. **(C)** Motivation *vs.* anxiety (Hyponeophagia). *Dixdc1KO* mice begin eating significantly later (*left*) and spend significantly less time eating an unfamiliar food (*right*) than WT. **(D)** Social behavior (SIP). *Dixdc1KO* mice spend significantly less time interacting with each other than *WT* (*left*). This reduction corresponds to significantly decreased average time per interaction (*middle*) and a reduced longest interaction (*right*).

(**E-Q**) Dendritic Spine Phenotypes. **(E)** Representative micrographs, primary dendrites from *WT* (top) and *KO* (bottom) cultured hippocampal neurons transfected with GFP; arrow, representative mature spine; asterisk, representative filopodia. **(F, G)** Quantification of spine density (**F**) and % spines with filopodial morphology (**G**) as visualized in (**E**). **(H)** Representative micrographs of cortical L5/6 apical dendrites from *WT* (top) and *KO* (bottom) visualized by GFP (*Tg(Thy1-EGFP)M)*; arrow, representative mature spine; asterisk, representative filopodia. **(I, J)** Quantification in L5/6 of spine density (**I**) and % immature spines (**J**) as visualized in (**H**). **(K-M)** Imaging of spine density and spine dynamics *in vivo*. (**K**) Representative 2-photon imaging of the same dendritic branch over 7 days in the primary somatosensory cortex of a one month old mouse; *WT* (top) and *KO* (bottom) visualized via YFP fluorescence (*Tg(Thy1-YFP)H*). (**L**) Quantification of spine density as visualized in (**K**). (**M**) Quantification of eliminated spines (arrows in **K**) and newly formed spines (arrowhead in **K**). **(N, O)** Decreased

hyperpolarization activated current (h-current; I_h) in *Dixdc1KO* mice. (**N**) Representative whole cell current clamp recordings in L5/6 prefrontal corticothalamic neurons. (**O**) Quantification of I_h as the sum of the initial voltage "sag" plus the magnitude of the after depolarization (ADP) following a hyperpolarizing current pulse. **(P)** Representative micrographs of cortical L5/6 apical dendrites in *WT* (top) and *KO* (bottom) visualized by GFP (*Tg(Thy1-EGFP)M)*; far red, hyperpolarization-activated cyclic nucleotide-gated channel 1 (HCN1). **(Q)** Quantification of HCN1-labelled spine density as visualized in (**P**). (**R-U**) Glutamatergic Synapse Phenotypes. **(R)** Representative micrographs, cultured hippocampal neurons from *WT* (top) *vs. Dixdc1KO* (bottom) transfected with GFP; green, GFP-filled primary dendrite; *blue*, VGLUT; *red*, PSD95; arrowheads, representative colocalized green/blue/red puncta (glutamatergic synapses). **(S)** Quantification of glutamatergic synapse density as visualized in (**R**). **(T)** Representative micrographs of cortical L5/6 apical dendrites in *WT* (top) and *KO* (bottom) visualized by GFP (*Tg(Thy1-EGFP)M)*; blue, VGLUT; *red*, PSD95; arrowheads, colocalized green/blue/red puncta (glutamatergic synapses). **(U)** Quantification of glutamatergic synapse density as visualized in (**T**).

Scale bars, 5 µm. * = *p<.05;* ** = *p<.01;* *** = *p<.001*

Figure 2.2
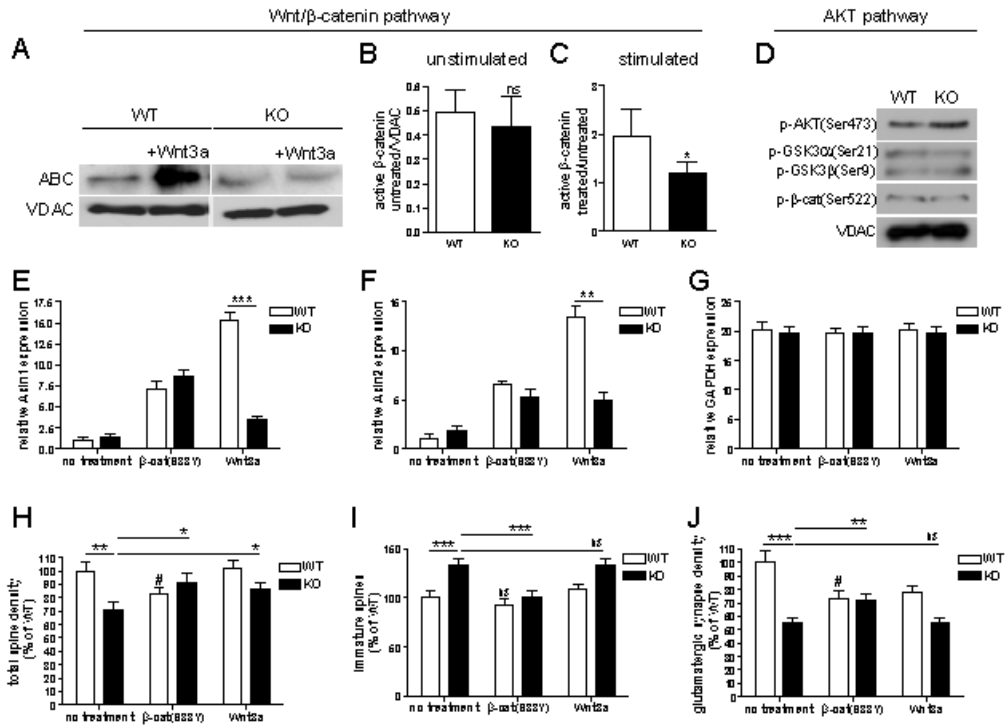
Figure 2.2. Decreased Wnt/β-catenin Signal Transduction in *Dixdc1KO* Neurons

(A) Immunoblot of active β-catenin ("ABC"; specifically unphosphorylated at S33) from cultured forebrain neurons (DIV18) either unstimulated or stimulated with Wnt3a.

(B) Quantification of active β-catenin from neurons not stimulated by Wnt3a shows no differences between *WT* and *Dixdc1KO.*

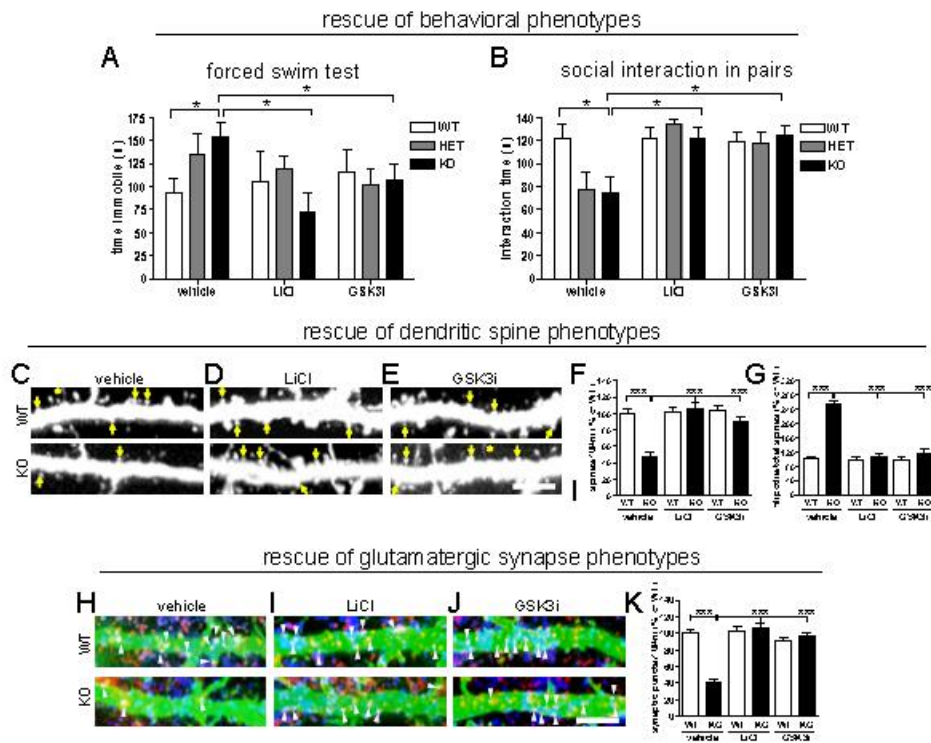**(C)** Stimulation by Wnt3a increases active β-catenin in *WT* but not in *Dixdc1KO* neurons.

(D) No detectable differences in phosphorylated AKT (p-AKT(Ser473)), nor in AKT-phosphorylated forms of: GSK3 (p-GSK3α(Ser21) top, p-GSK3β(Ser9) bottom) or β-catenin (p-β-cat(Ser522)), in *Dixdc1KO* neurons.

(E-G) Q-RT-PCR for Wnt/β-catenin pathway target genes *Axin1* (**E**) and *Axin2* (**F**), compared to control gene *GAPDH* (**G**), in cultured forebrain neurons (DIV18). Levels of Wnt/β-catenin pathway targets are not significantly different from WT in unstimulated *Dixdc1KO* neurons (left; black *vs.* white). These transcriptional targets respond normally to activation by a point-mutant stabilized form of β-catenin (middle; black *vs.* white). Transcription of these targets is significantly impaired in *Dixdc1KO* neurons downstream of Wnt3a (right; black *vs.* white).

(H-J) Quantification of total spine density (**H**), % immature spines (**I**) and glutamatergic synapse density (**J**) as in **Fig 1E-G**; **R**, **S** in *Dixdc1KO* (black) and *WT* (white) cultured hippocampal neurons: untreated (left), transfected with β-cat(S33Y) (middle), or treated with Wnt3a (right).

 * = *p<.05;* ** = *p<.01;* *** = *p<.001;* # = p<.05 *vs.* untransfected WT

Figure 2.3

rescue of behavioral phenotypes

A   forced swim test   B   social interaction in pairs

rescue of dendritic spine phenotypes

C vehicle   D LiCl   E GSK3i   F   G

rescue of glutamatergic synapse phenotypes

H vehicle   I LiCl   J GSK3i   K

Figure 2.3. GSK3 Inhibition Rescues *Dixdc1KO* Phenotypes

(A-B) Pharmacologic Rescue of Behavioral Phenotypes. The FST phenotype (increased time immobile) **(A)** and the SIP phenotype (reduced social interaction) **(B)** in *Dixdc1KO* mice is rescued by injection of either lithium or GSK3i.

(**C-G**) Pharmacologic Rescue of Dendritic Spine Phenotypes. **(C-E)** Representative micrographs of cortical L5/6 neurons from *WT* (top) and *KO* (bottom) treated with vehicle (**C**), lithium (**D**) or GSK3i (**E**), visualized by GFP (*Tg(Thy1-EGFP)M)*; arrow, representative mature spine; asterisk, representative filopodia. **(F, G)** Quantification of spine density (**F**) and % immature spines (**G**).

(H-K) Pharmacologic Rescue of Glutamatergic Synapse Phenotypes. (**H-J**) Representative micrographs of cortical L5/6 neurons from *WT* (top) and *KO* (bottom) treated with vehicle (**H**), lithium (**I**) or GSK3i (**J**), visualized by GFP (*Tg(Thy1-EGFP)M)*; blue, VGLUT; *red*, PSD95; arrowheads, co-localized green/blue/red puncta (glutamatergic synapses). **(K)** Quantification. Scale bars, 5µm. * = *p<.05;* ** *= p<.01;* *** *= p<.001*

Figure 2.4
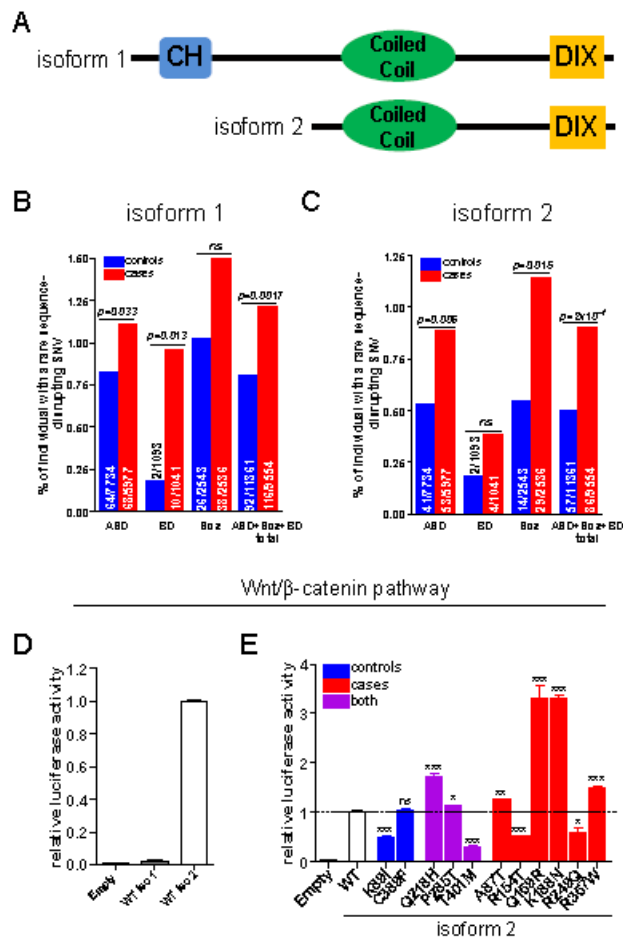
**Figure 2.4. Increased Rare *DIXDC1* SNVs with Functional Effects on Wnt/β-catenin Signaling in ASD, BD and Scz**

(A) Schematic representation of human DIXDC1 isoform 1 and isoform 2. Blue, calponin homology domain (CH); green, coiled-coil domain; yellow, DIX domain.

(B, C) % of individuals carrying a rare sequence-disrupting SNV in *DIXDC1* isoform 1 (**B**) and 2 (**C**).

(D) TOPflash (cell-based Wnt/β-catenin signaling assay) for human DIXDC1 isoform 1 and isoform 2. Values are normalized to WT DIXDC1 isoform 2 (white bar). Isoform 1 does not activate Wnt signaling in this assay.

(E) TOPflash for human *DIXDC1* alleles. Values are normalized to WT DIXDC1 isoform 2 (white bar). Blue bars indicate SNVs found only in unaffected controls in our combined datasets (n = 11361), red bars indicate SNVs found only in psychiatric cases in our combined datasets (n= 9554); purple bars indicate SNVs found in both cases and controls.

Figure 2.5

rescue of KO neurodevelopmental deficits   dominant neurodevelopmental deficits
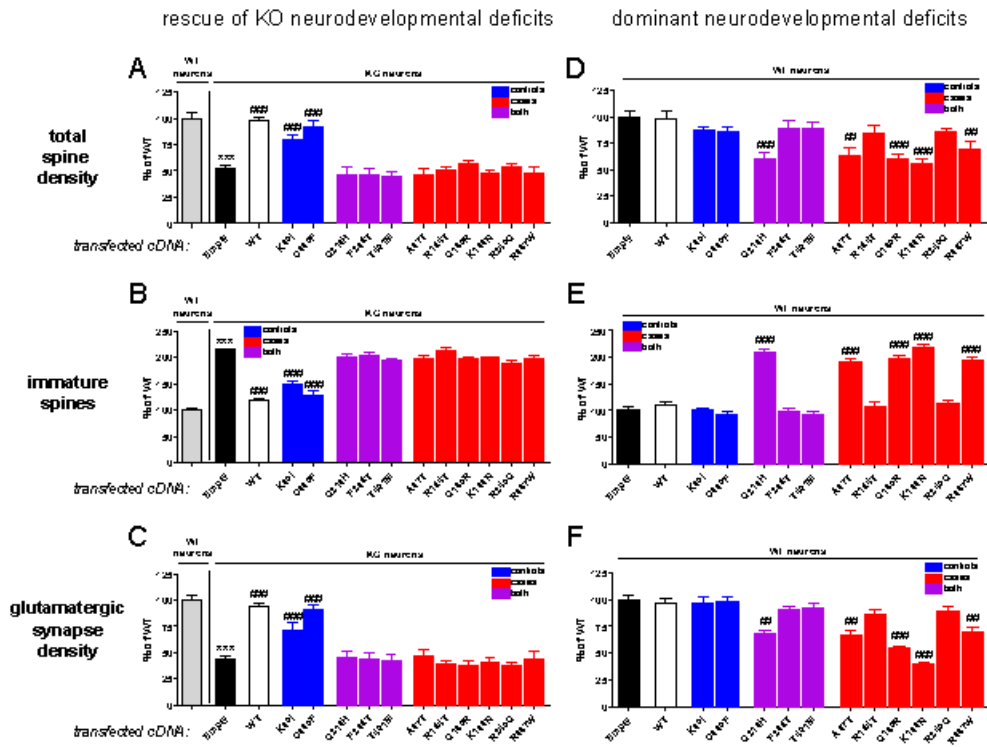
Figure 2.5. Rescue and Dominant Neurodevelopmental Effects of DIXDC1 SNVs

(A-C) Rescue. Recombinant expression of WT DIXDC1 isoform 2 in *Dixdc1KO* neurons (*white bars*) restores spine density (**A**), % immature spines (**B**) and glutamatergic synapse density (**C**) to WT levels (*grey bars*). Two control-derived DIXDC1 SNVs (K89I, C389F) (*blue bars*), but none of the SNVs found in patients (*purple & red bars*), rescue these phenotypes.

(D-F) Dominant Effects. Recombinant expression of a WT human DIXDC1 isoform 2 cDNA (white bars), or cDNAs containing Wnt/β-catenin pathway activity-neutral or -hypoactivating SNVs (K89I, R154T, R249Q, P285T, C389F, T401M) has no effect on neurodevelopmental phenotypes in WT neurons. In contrast, recombinant expression of cDNAs containing hyperactivating SNVs (A87T, Q169R, K188N, Q218H or R367W) in WT neurons leads to significant decreases in spine density (**D**), increased immature spine % (**E**) and glutamatergic synapse density (**F**).

*** = *p<.001 vs.* WT genotype in (**A-C**); **##** = *p<.01;* **###** = *p<.001 vs.* identical genotype transfected with empty vector in (**A-F**).

Supplementary Tables and Figures

Table 2.S1

| Behavior	Assay	Results
Locomotor activity	Open field	Normal
Complex behavior	Nest building	Normal-increased
Motor	Rotarod	Normal
Repetitive behavior	Digging/grooming/rearing	Normal
	Marble burying	Normal
Working memory	Y-maze	Normal
Aggressiveness	Tube test	Normal
Sociability	3-chambered box	Normal
	Interactions in pairs	**Decreased**-reversed by *LiCl and GSK3 inhibitor*
Anxiety	O-maze	Normal
	Center vs surround	**Increased**
	Hyponeophagia	**Increased**
Depression	Forced swim test	**Increased**-*reversed by LiCl and GSK3 inhibitor*
	Tail suspension test	Increased (trend)

Table S1. Behavioral assay results in *Dixdc1*KO mice (CD-1 genetic background)

Figure 2.S1
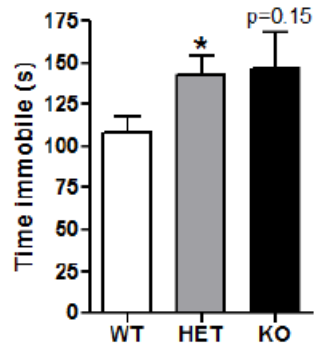
Figure S1. Depression-like behavior in the Tail Suspension Test. Dixdc1-/+ (HET) and -/- (KO) mice spend increased time immobile compared to +/+ (WT) littermates. * = *p<.05*

Figure 2.S2
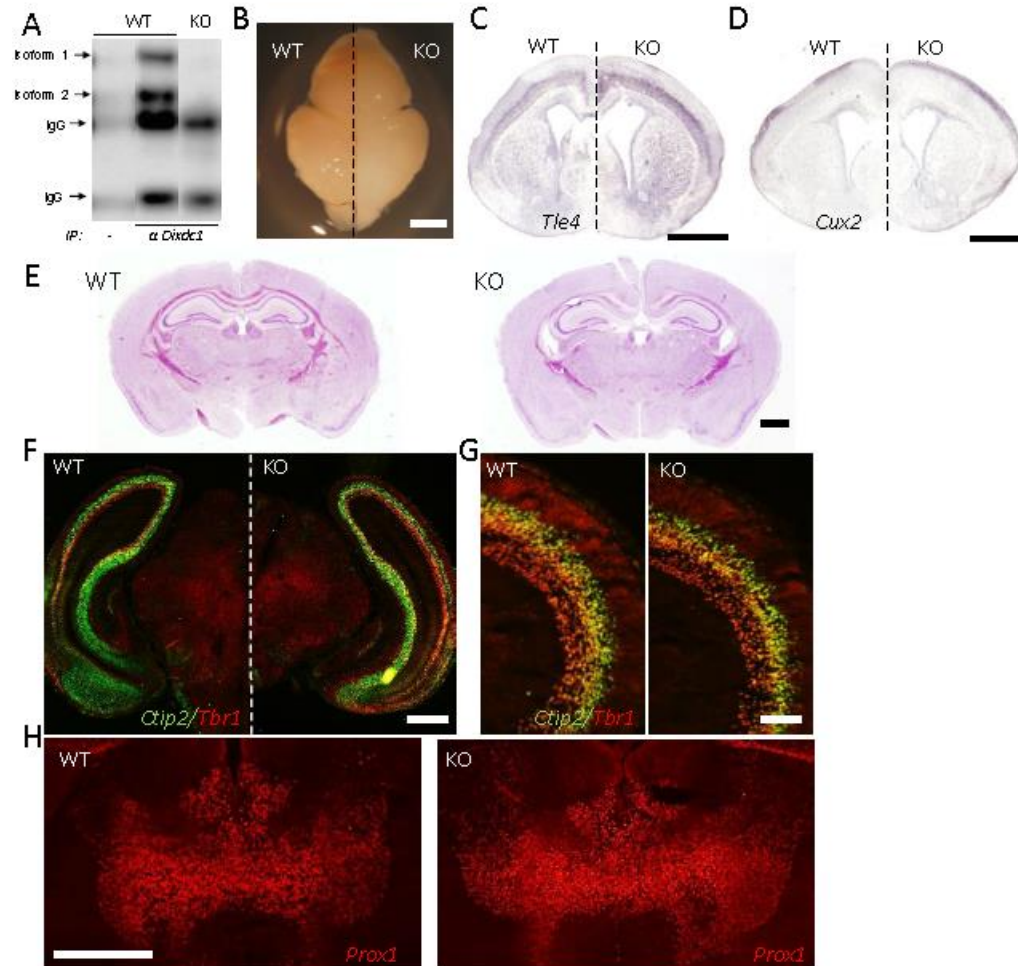
Figure S2.

(A) Immunoblot for Dixdc1 in neonatal WT and *Dixdc1KO* forebrain lysates immunoprecipitated (IP) with anti-Dixdc1 antibody. In WT (middle) both Dixdc1 isoform 1 (top band) and 2 (bottom band) are detected; in *Dixdc1KO* neither isoform is detected (right). No-antibody control (left) performed in parallel with no antibody added to the IP.

(B) Neonatal brains; left WT, right *Dixdc1KO*. Scale bar, 1mm.

(C-D) in situ hybridization for Tle4 (**b**) and Cux2 (**c**), neonatal coronal brain sections. Scale bar, 1mm

(E) Nissl staining of P30 coronal brain sections. Scale bar, 1mm.

(F,G) Late embryonic (embryonic day 18.5) coronal brain sections immunostained with antibodies for CTIP2 (green) and Tbr1 (red) for neurons migrating to cortical L5/L6. Scale bar in F, 500μm. Scale bar in G,150μm.

(H) P0 coronal brain sections showing thalamic neurons immunolabeled with Prox1. Scale bar, 1mm.

Figure 2.S3
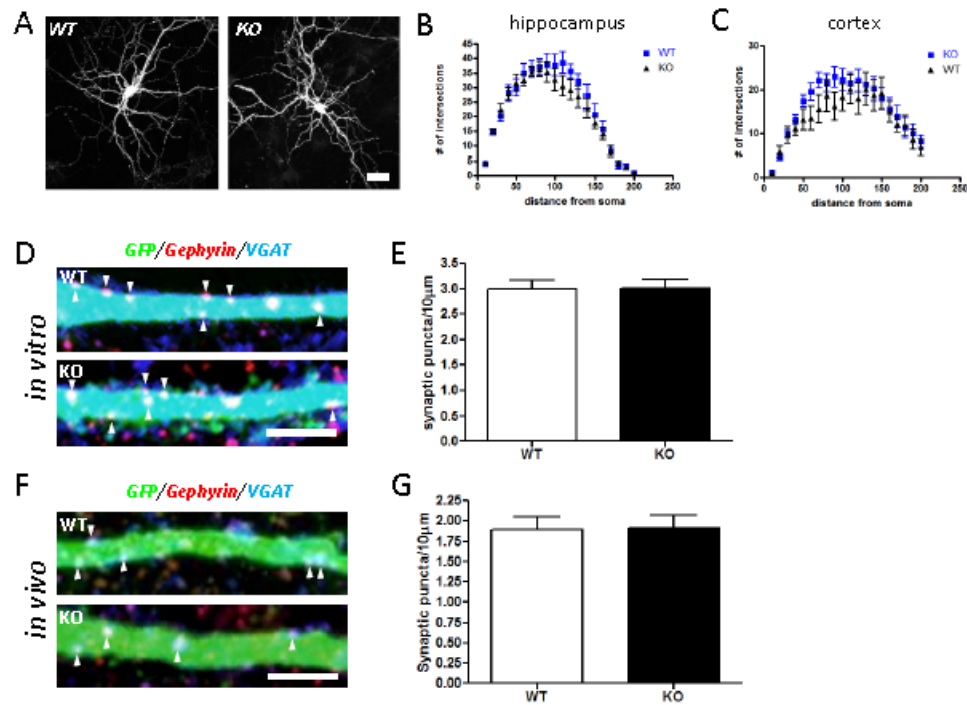
Supplemental Figure S3. Normal dentrite complexity and inhibitory synapses in *Dixdc1KO* neurons.
(A) GFP expressing cultured hippocampal pyramidal neurons (DIV18). Scale bar=30µm.
(B, C) Sholl analysis of cultured hippocampal (b) and cortical (c) pyramidal neurons.
(D) Representative micrographs of cultured hippocampal neurons (DIV18) immunolabeled for GFP (dendrite), VGAT (inhibitory presynapse) and gephyrin (inhibitory postsynapse). Scale bar, 5µm.
(E) Quantification of inhibitory (GABAergic) synapses (co-localized GFP, VGAT and gephyrin).
(F) Representative micrographs (P30 cortex) immunolabeled for GFP (dendrite), VGAT (inhibitory presynapse) and gephyrin (inhibitory postsynapse). Scale bar, 5µm.
(G) Quantification of inhibitory (GABAergic) synapses (co-localized GFP, VGAT and gephyrin).

Figure 2.S4
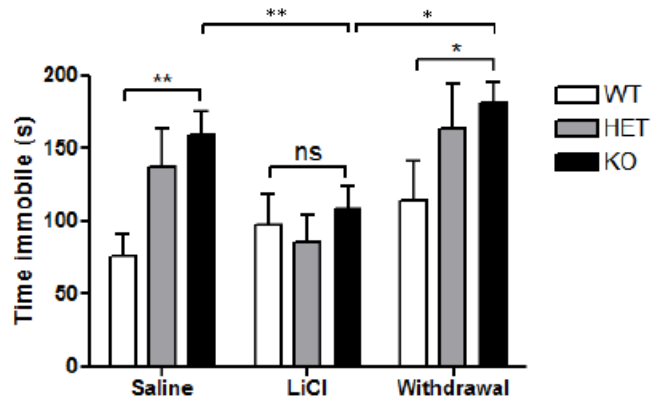
Figure S4. Withdrawal of lithium leads to behavioral relapse in the FST. Increased time immobile in *Dixdc1KO* mice is rescued by systemic injection of lithium (middle bars), compared to vehicle injected animals (left bars). Withdrawal of lithium for 14 days (right bars) leads to behavioral relapse. $* = p<.05$; $** = p<.01$

Figure 2.S5
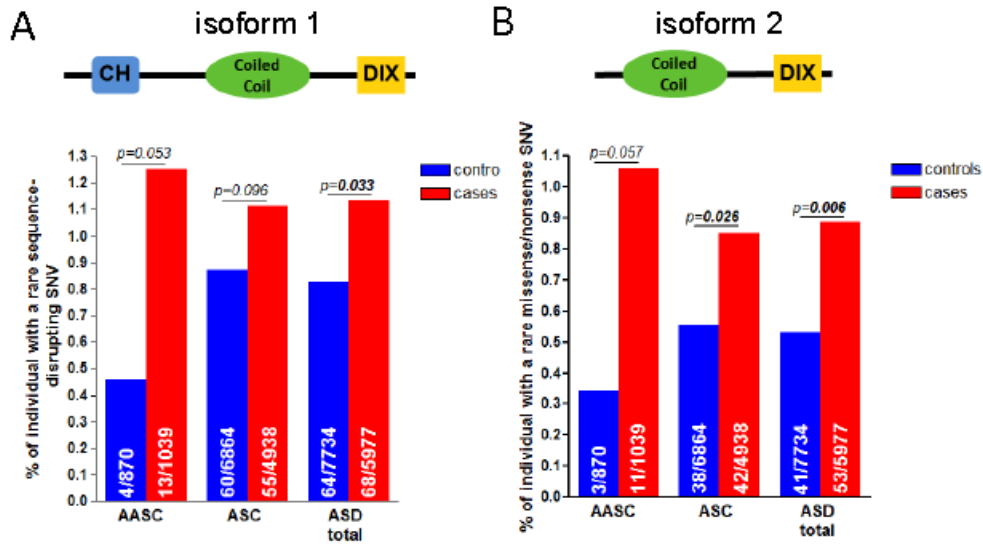
Figure S5. Increased burden of rare missense, nonsense and splice-disrupting SNVs in ASD from both the discovery (AASC) and replication (ASC) datasets in isoform 1 (A) and isoform 2 (B).

REFERENCES

Alimohamad, H., Sutton, L., Mouyal, J., Rajakumar, N., and Rushlow, W.J. (2005). The effects of antipsychotics on beta-catenin, glycogen synthase kinase-3 and dishevelled in the ventral midbrain of rats. J Neurochem *95*, 513-525.

Arguello, A., Yang, X., Vogt, D., Stanco, A., Rubenstein, J.L., and Cheyette, B.N. (2013). Dapper antagonist of catenin-1 cooperates with Dishevelled-1 during postsynaptic development in mouse forebrain GABAergic interneurons. PLoS One *8*, e67679.

Biechele, T.L., and Moon, R.T. (2008). Assaying beta-catenin/TCF transcription with beta-catenin/TCF transcription-based reporter constructs. Methods Mol Biol *468*, 99-110.

Chadman, K.K., Gong, S., Scattoni, M.L., Boltuck, S.E., Gandhy, S.U., Heintz, N., and Crawley, J.N. (2008). Minimal aberrant behavioral phenotypes of neuroligin-3 R451C knockin mice. Autism Res *1*, 147-158.

Ciani, L., Krylova, O., Smalley, M.J., Dale, T.C., and Salinas, P.C. (2004). A divergent canonical WNT-signaling pathway regulates microtubule dynamics: dishevelled signals locally to stabilize microtubules. JCell Biol *164*, 243-253.

Cryan, J.F., Valentino, R.J., and Lucki, I. (2005). Assessing substrates underlying the behavioral effects of antidepressants using the modified rat forced swimming test. Neurosci Biobehav Rev *29*, 547-569.

De Rubeis, S., He, X., Goldberg, A.P., Poultney, C.S., Samocha, K.E., Cicek, A.E., Kou, Y., Liu, L., Fromer, M., Walker, E.M.*, et al.* (2014). Synaptic, transcriptional and chromatin genes disrupted in autism. Nature.

Deacon, R.M. (2006). Digging and marble burying in mice: simple methods for in vivo identification of biological impacts. Nat Protoc *1*, 122-124.

Deacon, R.M. (2011). Hyponeophagia: a measure of anxiety in the mouse. J Vis Exp.

Duman, R.S. (2014). Pathophysiology of depression and innovative treatments: remodeling glutamatergic synaptic connections. Dialogues Clin Neurosci *16*, 11-27.

Feng, G., Mellor, R.H., Bernstein, M., Keller-Peck, C., Nguyen, Q.T., Wallace, M., Nerbonne, J.M., Lichtman, J.W., and Sanes, J.R. (2000). Imaging neuronal subsets in transgenic mice expressing multiple spectral variants of GFP. Neuron *28*, 41-51.

Goodwin, J.M., Svensson, R.U., Lou, H.J., Winslow, M.M., Turk, B.E., and Shaw, R.J. (2014). An AMPK-independent signaling pathway downstream of the LKB1 tumor suppressor controls Snail1 and metastatic potential. Mol Cell *55*, 436-450.

Hall, A.C., Lucas, F.R., and Salinas, P.C. (2000). Axonal remodeling and synaptic differentiation in the cerebellum is regulated by WNT-7a signaling. Cell *100*, 525-535.

Hayashi-Takagi, A., Takaki, M., Graziane, N., Seshadri, S., Murdoch, H., Dunlop, A.J., Makino, Y., Seshadri, A.J., Ishizuka, K., Srivastava, D.P.*, et al.* (2010). Disrupted-in-Schizophrenia 1 (DISC1) regulates spines of the glutamate synapse via Rac1. Nat Neurosci *13*, 327-332.

Hedgepeth, C.M., Conrad, L.J., Zhang, J., Huang, H.C., Lee, V.M., and Klein, P.S. (1997). Activation of the Wnt signaling pathway: a molecular mechanism for lithium action. Dev Biol *185*, 82-91.

Higgins, G.A., Allyn-Feuer, A., Barbour, E., and Athey, B.D. (2015). A glutamatergic network mediates lithium response in bipolar disorder as defined by epigenome pathway analysis. Pharmacogenomics *16*, 1547-1563.

Ikeuchi, Y., Stegmuller, J., Netherton, S., Huynh, M.A., Masu, M., Frank, D., Bonni, S., and Bonni, A. (2009). A SnoN-Ccd1 pathway promotes axonal morphogenesis in the mammalian brain. J Neurosci *29*, 4312-4321.

Iossifov, I., O'Roak, B.J., Sanders, S.J., Ronemus, M., Krumm, N., Levy, D., Stessman, H.A., Witherspoon, K., Vives, L., Patterson, K.E.*, et al.* (2014). The contribution of de novo coding mutations to autism spectrum disorder. Nature.

Jamain, S., Radyushkin, K., Hammerschmidt, K., Granon, S., Boretius, S., Varoqueaux, F., Ramanantsoa, N., Gallego, J., Ronnenberg, A., Winter, D.*, et al.* (2008). Reduced social interaction and ultrasonic communication in a mouse model of monogenic heritable autism. Proc Natl Acad Sci U S A *105*, 1710-1715.

Kalkman, H.O. (2012). A review of the evidence for the canonical Wnt pathway in autism spectrum disorders. Mol Autism *3*, 10.

Kerr, K.S., Fuentes-Medel, Y., Brewer, C., Barria, R., Ashley, J., Abruzzi, K.C., Sheehan, A., Tasdemir-Yilmaz, O.E., Freeman, M.R., and Budnik, V. (2014). Glial wingless/Wnt regulates glutamate receptor clustering and synaptic physiology at the Drosophila neuromuscular junction. J Neurosci *34*, 2910-2920.

Kivimae, S., Martin, P.M., Kapfhamer, D., Ruan, Y., Heberlein, U., Rubenstein, J.L., and Cheyette, B.N. (2011). Abnormal behavior in mice mutant for the Disc1 binding partner, Dixdc1. Transl Psychiatry *1*, e43.

Koike, H., Arguello, P.A., Kvajo, M., Karayiorgou, M., and Gogos, J.A. (2006). Disc1 is mutated in the 129S6/SvEv strain and modulates working memory in mice. Proc Natl Acad Sci U S A *103*, 3693-3697.

Kondratiuk, I., Leski, S., Urbanska, M., Biecek, P., Devijver, H., Lechat, B., Van Leuven, F., Kaczmarek, L., and Jaworski, T. (2016). GSK-3beta and MMP-9 Cooperate in the Control of Dendritic Spine Morphology. Mol Neurobiol.

Krumm, N., O'Roak, B.J., Shendure, J., and Eichler, E.E. (2014). A de novo convergence of autism genetics and molecular neuroscience. Trends Neurosci *37*, 95-105.

Kwan, V., Hung, C., Holzapfel, N., Walker, S., Murtaza, N., Unda, B., White, S., Yuen, R.K.C., Habing, K., Milson, C., *et al.* (2016). DIXDC1 phosphorylation and control of dendrite morphology is impaired by rare genetic variants. Neuron, submitted 21016.

Lenox, R.H., and Wang, L. (2003). Molecular basis of lithium action: integration of lithium-responsive signaling and gene expression networks. Mol Psychiatry *8*, 135-144.

Liu, R.J., Fuchikami, M., Dwyer, J.M., Lepack, A.E., Duman, R.S., and Aghajanian, G.K. (2013). GSK-3 inhibition potentiates the synaptogenic and antidepressant-like effects of subthreshold doses of ketamine. Neuropsychopharmacology *38*, 2268-2277.

Liu, Y.T., Dan, Q.J., Wang, J., Feng, Y., Chen, L., Liang, J., Li, Q., Lin, S.C., Wang, Z.X., and Wu, J.W. (2011). Molecular basis of Wnt activation via the DIX domain protein Ccd1. J Biol Chem *286*, 8597-8608.

Long, J.M., LaPorte, P., Paylor, R., and Wynshaw-Boris, A. (2004). Expanded characterization of the social interaction abnormalities in mice lacking Dvl1. Genes Brain Behav *3*, 51-62.

Luo, W., Zou, H., Jin, L., Lin, S., Li, Q., Ye, Z., Rui, H., and Lin, S.C. (2005). Axin contains three separable domains that confer intramolecular, homodimeric, and heterodimeric interactions involved in distinct functions. J Biol Chem *280*, 5054-5060.

Martin, P.M., Yang, X., Robin, N., Lam, E., Rabinowitz, J.S., Erdman, C.A., Quinn, J., Weiss, L.A., Hamilton, S.P., Kwok, P.Y.*, et al.* (2013). A rare WNT1 missense variant overrepresented in ASD leads to increased Wnt signal pathway activation. Transl Psychiatry *3*, e301.

McKenna, A., Hanna, M., Banks, E., Sivachenko, A., Cibulskis, K., Kernytsky, A., Garimella, K., Altshuler, D., Gabriel, S., Daly, M.*, et al.* (2010). The Genome Analysis Toolkit: a MapReduce framework for analyzing next-generation DNA sequencing data. Genome Res *20*, 1297-1303.

Mohn, J.L., Alexander, J., Pirone, A., Palka, C.D., Lee, S.Y., Mebane, L., Haydon, P.G., and Jacob, M.H. (2014). Adenomatous polyposis coli protein deletion leads to cognitive and autism-like disabilities. Mol Psychiatry *19*, 1133-1142.

Moon, R.T., Brown, J.D., and Torres, M. (1997). WNTs modulate cell fate and behavior during vertebrate development. Trends Genet *13*, 157-162.

Mulligan, K.A., and Cheyette, B.N. (2012). Wnt signaling in vertebrate neural development and function. J Neuroimmune Pharmacol *7*, 774-787.

Musazzi, L., Treccani, G., Mallei, A., and Popoli, M. (2013). The action of antidepressants on the glutamate system: regulation of glutamate release and glutamate receptors. Biol Psychiatry *73*, 1180-1188.

Nurnberger, J.I.J., DePaulo, J.R., Gershon, E.S., Reich, T., Blehar, M.C., Edenberg, H.J., Foroud, T., Miller, M., Bowman, E., Mayeda, A.*, et al.* (1997). Genomic survey of bipolar illness in the NIMH genetics initiative pedigrees: a preliminary report. Am J Med Genet *74*, 227-237.

O'Brien, W.T., and Klein, P.S. (2009). Validating GSK3 as an in vivo target of lithium action. Biochem Soc Trans *37*, 1133-1138.

O'Roak, B.J., Vives, L., Girirajan, S., Karakoc, E., Krumm, N., Coe, B.P., Levy, R., Ko, A., Lee, C., Smith, J.D.*, et al.* (2012). Sporadic autism exomes reveal a highly interconnected protein network of de novo mutations. Nature *485*, 246-250.

Okerlund, N.D., Kivimae, S., Tong, C.K., Peng, I.F., Ullian, E.M., and Cheyette, B.N. (2010). Dact1 is a postsynaptic protein required for dendrite, spine, and excitatory synapse development in the mouse forebrain. J Neurosci *30*, 4362-4368.

Paspalas, C.D., Wang, M., and Arnsten, A.F. (2013). Constellation of HCN channels and cAMP regulating proteins in dendritic spines of the primate prefrontal cortex: potential substrate for working memory deficits in schizophrenia. Cereb Cortex *23*, 1643-1654.

Pinto, D., Delaby, E., Merico, D., Barbosa, M., Merikangas, A., Klei, L., Thiruvahindrapuram, B., Xu, X., Ziman, R., Wang, Z.*, et al.* (2014). Convergence of genes and cellular pathways dysregulated in autism spectrum disorders. Am J Hum Genet *94*, 677-694.

Porteous, D.J., Millar, J.K., Brandon, N.J., and Sawa, A. (2011). DISC1 at 10: connecting psychiatric genetics and neuroscience. Trends Mol Med *17*, 699-706.

Purcell, S.M., Moran, J.L., Fromer, M., Ruderfer, D., Solovieff, N., Roussos, P., O'Dushlaine, C., Chambert, K., Bergen, S.E., Kahler, A.*, et al.* (2014). A polygenic burden of rare disruptive mutations in schizophrenia. Nature *506*, 185-190.

Rothwell, P.E., Fuccillo, M.V., Maxeiner, S., Hayton, S.J., Gokce, O., Lim, B.K., Fowler, S.C., Malenka, R.C., and Sudhof, T.C. (2014). Autism-associated neuroligin-3 mutations commonly impair striatal circuits to boost repetitive behaviors. Cell *158*, 198-212.

Sanders, A.R., Duan, J., Levinson, D.F., Shi, J., He, D., Hou, C., Burrell, G.J., Rice, J.P., Nertney, D.A., Olincy, A.*, et al.* (2008). No significant association of 14 candidate genes with schizophrenia in a large European ancestry sample: implications for psychiatric genetics. Am J Psychiatry *165*, 497-506.

Sanders, S.J., He, X., Willsey, A.J., Ercan-Sencicek, A.G., Samocha, K.E., Cicek, A.E., Murtha, M.T., Bal, V.H., Bishop, S.L., Dong, S.*, et al.* (2015). Insights into Autism Spectrum Disorder Genomic Architecture and Biology from 71 Risk Loci. Neuron *87*, 1215-1233.

Sanders, S.J., Murtha, M.T., Gupta, A.R., Murdoch, J.D., Raubeson, M.J., Willsey, A.J., Ercan-Sencicek, A.G., DiLullo, N.M., Parikshak, N.N., Stein, J.L.*, et al.* (2012). De novo

mutations revealed by whole-exome sequencing are strongly associated with autism. Nature *485*, 237-241.

Sekar, A., Bialas, A.R., de Rivera, H., Davis, A., Hammond, T.R., Kamitaki, N., Tooley, K., Presumey, J., Baum, M., Van Doren, V.*, et al.* (2016). Schizophrenia risk from complex variation of complement component 4. Nature.

Shiomi, K., Kanemoto, M., Keino-Masu, K., Yoshida, S., Soma, K., and Masu, M. (2005). Identification and differential expression of multiple isoforms of mouse Coiled-coil-DIX1 (Ccd1), a positive regulator of Wnt signaling. Brain Res Mol Brain Res *135*, 169-180.

Shiomi, K., Uchida, H., Keino-Masu, K., and Masu, M. (2003). Ccd1, a novel protein with a DIX domain, is a positive regulator in the Wnt signaling during zebrafish neural patterning. Curr Biol *13*, 73-77.

Shorter, E. (2009). The history of lithium therapy. Bipolar Disord *11 Suppl 2*, 4-9.

Singh, K.K., Ge, X., Mao, Y., Drane, L., Meletis, K., Samuels, B.A., and Tsai, L.H. (2010). Dixdc1 is a critical regulator of DISC1 and embryonic cortical development. Neuron *67*, 33-48.

Soma, K., Shiomi, K., Keino-Masu, K., and Masu, M. (2006). Expression of mouse Coiled-coil-DIX1 (Ccd1), a positive regulator of Wnt signaling, during embryonic development. Gene Expr Patterns *6*, 325-330.

Svenningsson, P., Tzavara, E.T., Carruthers, R., Rachleff, I., Wattler, S., Nehls, M., McKinzie, D.L., Fienberg, A.A., Nomikos, G.G., and Greengard, P. (2003). Diverse psychotomimetics act through a common signaling pathway. Science *302*, 1412-1415.

Tan, C., Qiao, F., Wei, P., Chi, Y., Wang, W., Ni, S., Wang, Q., Chen, T., Sheng, W., Du, X.*, et al.* (2015). DIXDC1 activates the Wnt signaling pathway and promotes gastric cancer cell invasion and metastasis. Mol Carcinog.

Wang, L., Li, H., Chen, Q., Zhu, T., Zhu, H., and Zheng, L. (2009). Wnt signaling stabilizes the DIXDC1 protein through decreased ubiquitin-dependent degradation. Cancer Sci *101*, 700-706.

Wang, X., Zheng, L., Zeng, Z., Zhou, G., Chien, J., Qian, C., Vasmatzis, G., Shridhar, V., Chen, L., and Liu, W. (2006). DIXDC1 isoform, l-DIXDC1, is a novel filamentous actin-binding protein. Biochem Biophys Res Commun *347*, 22-30.

Wong, C.K., Luo, W., Deng, Y., Zou, H., Ye, Z., and Lin, S.C. (2004). The DIX domain protein coiled-coil-DIX1 inhibits c-Jun N-terminal kinase activation by Axin and dishevelled through distinct mechanisms. J Biol Chem *279*, 39366-39373.

Xu, T., Yu, X., Perlik, A.J., Tobin, W.F., Zweig, J.A., Tennant, K., Jones, T., and Zuo, Y. (2009). Rapid formation and selective stabilization of synapses for enduring motor memories. Nature *462*, 915-919.

Xu, Z., Liu, D., Fan, C., Luan, L., Zhang, X., and Wang, E. (2014). DIXDC1 increases the invasion and migration ability of non-small-cell lung cancer cells via the PI3K-AKT/AP-1 pathway. Mol Carcinog *53*, 917-925.

Zhang, Y., Chen, K., Sloan, S.A., Bennett, M.L., Scholze, A.R., O'Keeffe, S., Phatnani, H.P., Guarnieri, P., Caneda, C., Ruderisch, N.*, et al.* (2014). An RNA-sequencing transcriptome and splicing database of glia, neurons, and vascular cells of the cerebral cortex. J Neurosci *34*, 11929-11947.

Zhou, X.L., Giacobini, M., Anderlid, B.M., Anckarsater, H., Omrani, D., Gillberg, C., Nordenskjold, M., and Lindblom, A. (2007). Association of adenomatous polyposis coli (APC) gene polymorphisms with autism spectrum disorder (ASD). Am J Med Genet B Neuropsychiatr Genet *144B*, 351-354.

Chapter 3

The Planar Cell Polarity transmembrane protein Vangl2 promotes dendrite, spine and excitatory synapse formation in the mammalian forebrain

Summary

The transmembrane protein Vangl2, a key regulator of the Wnt/Planar Cell Polarity (PCP) pathway, is involved in dendrite arbor elaboration, dendritic spine formation and glutamatergic synapse formation in mammalian central nervous system neurons. Two genetic mouse models were used in this study- a constitutive *Vangl2* knockout and a mutant *Looptail (lp) Vangl2*, both of which are homozygous embryonic lethal. Cultured forebrain neurons from Vangl2 knockout mice have simpler dendrite arbors, fewer total spines, less mature spines and fewer glutamatergic synapse inputs on their dendrites than control neurons. Neurons from mice heterozygous for the semi-dominant *Vangl2 lp* mutation have similar but not identical phenotypes and these phenotypes are also observed in Golgi-stained brain tissue from adult mutant mice. Given increasing evidence linking psychiatric pathophysiology to these sub-neuronal sites and structures, our findings underscore the relevance of core PCP signaling proteins including Vangl2 to the underlying biology of major mental illnesses and their treatment.

Introduction

Dendrite, dendritic spine and excitatory (glutamatergic) synapse formation and plasticity are molecularly interrelated developmental prerequisites for proper brain function and behavior. Defects in spine and synapse formation and turnover are increasingly

understood to be key contributors to neuropsychiatric disorders including autism, schizophrenia and major affective disorders [1-5].

Cell communication pathways with well-established roles in other aspects of development – including both the Wnt/β-catenin pathway [6-8] and the Wnt/Planar Cell Polarity (PCP) pathway [9-11] - participate in these processes. The four-pass transmembrane protein Van Gogh-like 2 (Vangl2) is a key player in the PCP pathway and it interacts with several proteins that influence synapse formation, including other PCP proteins such as Dishevelled (Dvl) [12] and Dapper-antagonist of catenin-1 (Dact1) [13] as well as the postsynaptic protein PSD95 [14-16]. Vangl2 also participates in signaling upstream of small GTPases [17, 18] regulating cytoskeletal dynamics crucial to dendrite and dendritic spine formation and plasticity [19-22]. *Looptail* (*Lp*) is a missense mutation in *Vangl2* [23] that causes semidominant phenotypes reflective of abnormal PCP including, in heterozygous animals, the curled or kinked tail from which the mutation gets its name, and in homozygous animals, craniorachischesis, a completely open neural tube and exposed brain [23-25]. Genetically-engineered *null* mutations in Vangl2 cause similar phenotypes, but recessively and with lower penetrance in homozygous mutant animals [26, 27]. Using both allele types, we show here that Vangl2 functions during neural differentiation in dendrite arborization, spine formation, spine maturation and glutamatergic synapse formation.

Methods

Genetics The *Vangl2$^\Delta$* allele [26] is here referred to as *Vangl2KO* or *Vangl2$^-$*. The *Ltap^{Lp}* allele (Jackson Laboratory stock number 000220) [23] is here referred to as *Vangl2^{Lp}* or

Lp. All assays compared littermates of the designated experimental and control genotypes derived from *Vangl2*$^{-/+}$ or *Vangl2*$^{Lp/+}$ intercrosses.

Recombinant DNA

The mouse Vangl2 cDNA clone and expression plasmid has been described previously [28].

Primary Culture and Immunostaining

Dissociated neurons were obtained from embryos, fixed, transfected with pEGFP-C1 (Clontech) and immunostained for synaptic markers as previously described [29, 30]. Hippocampal cultures were used where possible because of the ease of producing populations of predominantly pyramidal neurons and prior validation as a model system relevant to dendrite, spine and synapse formation in the forebrain [31]. The borders of the hippocampus were not consistently identifiable in mutant homozygotes (both *Vangl2*$^{\Delta/\Delta}$ and *Vangl2*$^{Lp/Lp}$) due to craniorachischisis and neural precursor migration defects [27, 32]. Therefore, for these genotypes the entire forebrain (cortex and hippocampus) was prepared and compared to entire forebrain cultures of wild type (WT) and heterozygous littermates.

Visualization and Quantification

Cells were visualized on a Nikon CS1i upright spectral confocal at 40x magnification or a custom built spinning disc confocal microscope (Zeiss Axiovert 200M with Perkin-Elmer spinning disc and Melles Griot 43 series ion laser, Cascade 512B digital camera (Roper Scientific)) at 40x magnification. Golgi images were obtained on an Olympus IX51 compound inverted fluorescence microscope, also at 40x. Images were analyzed

with ImageJ software (NIH). Sholl analysis, dendritic spine binning and spine and synapse quantification were performed as previously described [30].

Golgi Staining

Golgi-Cox silver staining was performed on 4 month old littermates using the FD GolgiStain kit (FD Neurotechnologies) according to manufacturer's instructions.

Statistics

All *p* values were calculated by unpaired parametric t tests (2-way comparison) or one-way ANOVA (≥3 comparisons) with Tukey's post hoc analysis using Graphpad Prism software. Each comparison entailed ≥8 neurons and ≥11 dendrites per condition derived from multiple independent experiments; all reported differences reflect a minimal p≤0.05 for experimental *vs.* control.

Results

Genetic Elimination of Vangl2 Reduces Dendrite Arbor and Spine Formation

On inspection cultured *Vangl2$^{-/-}$* forebrain pyramidal neurons had simpler dendrite arbors than controls (**Fig 1A** *vs.* **B**). Sholl analysis confirmed that mutant neurons had reduced numbers of dendrite branch crossings (**Fig 1F**). The maturation and density of dendritic spines were also affected (**Fig 1A'** *vs.* **B'**): the density of spines along dendrites was lower in *Vangl2$^{-/-}$* neurons compared to WT (WT 2.9±0.4 *vs. Vangl2$^{-/-}$* 1.6±0.2, *p*=0.002; **Fig 1G**). Moreover, *Vangl2$^{-/-}$* neurons had an increased percentage of immature (*i.e.* filopodial) relative to mature (*i.e.* thin, mushroom or stub-shaped) spines (WT 10±2 *vs. Vangl2$^{-/-}$* 25±4, *p*=0.007; **Fig 1H**).

Recombinantly expression of Vangl2 rescued the dendrite arbor phenotype in *Vangl2*$^{-/-}$ neurons (**Fig 1C**, **F**). It also rescued spine density (spines/10μ in: rescued 2.0±0.2 *vs.* WT 2.9±0.4, *p*=0.07) and spine maturity (percent filopodia in: rescued 13±2 *vs.* WT 10±2, *p*>0.9; **Fig 1A'**, **C'**, **G**, **H**).

Vangl2 Overexpression and Heterozygosity do not alter Dendrites or Spines

To investigate effects of other genetic manipulations expected to alter (but not eliminate) Vangl2 levels, we examined phenotypes in WT neurons recombinantly overexpressing Vangl2, and also in heterozygous (*Vangl2*$^{-/+}$) neurons. Neither of these genetic manipulations had any effect on dendrite complexity (**Fig 1A** *vs.* **D** and **E**; **1F**), spine density (spines/10μ in: WT 2.9±0.4 *vs.* WT+Vangl2 2.6±0.3, *p*=0.9; *vs. Vangl2*$^{-/+}$ 2.6±0.3, *p*=0.8; **Fig 1A'** *vs.* **D'** and **E'**; **1G**) or spine maturity (percent filopodia in: WT 10±2 *vs.* WT+Vangl2 17±5, *p*=0.6; *vs. Vangl2*$^{-/+}$ 8±3, *p*>0.9; **Fig 1A'** *vs.* **D'** and **E'**; **1H**).

Vangl2$^{-/-}$ *Dendrites have Fewer Glutamatergic Synaptic Contacts*

We quantified density of glutamatergic synapses along dendrites by visualization with antibodies specific for VGlut1 (presynaptic marker) and PSD95 (postsynaptic marker). *Vangl2*$^{-/-}$ neurons had reduced glutamatergic synapse density (per 10μ in: WT 3.1±0.3 *vs. Vangl2*$^{-/-}$ 1.5±0.1, *p*<0.0001; **Fig 1I** *vs.* **J**; **1N**). Recombinant expression of Vangl2 in *Vangl2*$^{-/-}$ neurons rescued glutamatergic synapse density (per 10μ in: WT 3.1±0.3 *vs. Vangl2*$^{-/-}$+Vangl2 2.4±0.2, *p*=0.1; **Fig 1J** *vs.* **K**; **1N**). Neither WT neurons recombinantly overexpressing Vangl2 (**Fig 1L**) nor *Vangl2*$^{-/+}$ neurons (**Fig 1M**) were significantly different from WT in this assay (per 10μ in: WT 3.1±0.3 *vs.* WT+Vangl2 2.5±0.2, *p*=0.2;

vs. Vangl2$^{-/+}$ 3.0±0.3, *p*=0.9; **Fig 1N**). In contrast to this glutamatergic synapse

phenotype, *Vangl2$^{-/-}$* neurons had no significant reduction in inhibitory (GABAergic)

synapse density on their dendrites measured similarly (data not shown).

Lp Causes mixed effects on Dendrite Arbors, Spines and Glutamatergic Synapses

As with *Vangl2$^{-/-}$* neurons, upon visual inspection *Vangl2$^{Lp/+}$* neurons had simpler

dendrite arbors than WT (**Fig 2A**, **B**). Interestingly, although homozygous (*Vangl2$^{Lp/Lp}$*)

mice have more severe cell polarity phenotypes than heterozygous (*Vangl2$^{Lp/+}$*) mice in

embryonic axis elongation, inner ear epithelia, and neural precursor proliferation and

migration [26, 32], neurons from *Vangl2$^{Lp/Lp}$* mice did not have a greater decrease in

dendrite complexity than those from *Vangl2$^{Lp/+}$* mice (**Fig 2B**, **C**). Sholl analysis

revealed that *Lp* neurons, whether heterozygous or homozygous, had similar reductions

in number of dendrite branch crossings (**Fig 2F**). Dendritic spines were also affected by

the *Lp* mutation, not in terms of density (per 10μ in: WT 2.8±0.2 *vs. Vangl2$^{Lp/+}$* 2.3±0.2,

p=0.1; *vs. Vangl2$^{Lp/Lp}$* 2.6±0.2, *p*=0.6; **Fig 2A'**, **B'**, **C**; **2G**) but in terms of maturity

(percent filopodia in: WT 18±3 *vs. Vangl2$^{Lp/+}$* 34±3, *p*<0.0001; *vs. Vangl2$^{Lp/Lp}$* 33±4,

p<0.0001; **Fig 2H**).

   Similar to *Vangl2$^{-/-}$* neurons, glutamatergic synapse density along dendrites of

Vangl2$^{Lp/+}$ and *Vangl2 $^{Lp/Lp}$* neurons was reduced compared to WT (per 10μ in: WT

2.4±0.1 *vs. Vangl2$^{Lp/+}$* 1.4±0.1, *p*<0.0001; *vs. Vangl2 $^{Lp/Lp}$* 1.3±0.1, *p*<0.0001; **Fig 2I-K**;

2M). As in *Vangl2$^{-/-}$* neurons, GABAergic synapse density was unaffected (data not

shown).

Vangl2 Overexpression Rescues only some Lp Neurodevelopmental Phenotypes

As stated above, neurons carrying the *Vangl2^{Lp}* allele, whether heterozygous or homozygous, displayed similar decreases in dendrite complexity, spine maturation and glutamatergic synapse density. Interestingly, only the spine maturation phenotype was rescued by recombinant expression of Vangl2: Recombinant overexpression of Vangl2 did not rescue dendrite complexity (**Fig 2E**, **F**), nor did it rescue glutamatergic synapse density along dendrites in *Lp* mutant neurons (per 10µ in: WT 2.4±0.1 *vs.* *Vangl2$^{Lp/+}$*+Vangl2 1.3±0.1, *p*<0.0001; **Fig 2L**, **M**). In contrast, overexpression of WT Vangl2 did rescue spine maturity in these neurons (percent filopodia in: WT 18±3 *vs.* *Vangl2$^{Lp/+}$*+Vangl2 16±3, *p*>0.9; **Fig 2B'**, **D'**; **2H** blue *vs.* black bar).

Elimination of Dact1 does not Rescue Lp Neurodevelopmental Phenotypes

We previously showed that genetic loss of the Wnt signal pathway scaffold protein Dact1 can rescue embryonic phenotypes in *Vangl2$^{Lp/+}$*mice [13]. Dact1 is expressed in differentiating forebrain neurons and its loss causes reductions in dendrite arbor complexity, dendritic spine maturity and glutamatergic synapse formation [30] similar to the *Vangl2* mutant phenotypes reported here. Nonetheless, neurons from *Vangl2$^{Lp/+}$*; *Dact1$^{-/-}$* mice had no rescue of dendrite complexity (**Fig 2B** *vs.* **E**; **2F**) and no rescue of spine maturity (% filopodia in: *Vangl2$^{Lp/+}$*34±3 *vs. Vangl2$^{Lp/+}$*; *Dact1$^{-/-}$* 41±4, *p*=0.2; **Fig 2B'** *vs.* **E'**; **2H** orange *vs.* light grey bar) relative to *Vangl2$^{Lp/+}$* neurons.

Golgi Staining Confirms Spine Reductions in the Vangl2 Mutant Forebrain

75

All the preceding assays were conducted using cultured forebrain neurons. To confirm that similar phenotypes occur in intact mammalian forebrain tissue we analyzed morphology of pyramidal neurons in the CA1 region of the hippocampus via Golgi-Cox staining on brains taken from adult (4-6 month old) $Vangl2^{Lp/+}$ and littermate control mice. (The prenatal death of $Vangl2^{-/-}$ and $Vangl2^{Lp/Lp}$ mice precluded such analysis). CA1 pyramidal neurons in $Vangl2^{Lp/+}$ mice had decreased spine density on apical dendrites compared to controls (per unit length in: WT 7.6±0.7 *vs.* $Vangl2^{Lp/+}$ 4.6±0.6, p=0.005; **Fig 2N-P**). They also had an increased percentage of immature (filopodial) projections (WT 10±2 *vs.* $Vangl2^{Lp/+}$ 17±2, p=0.02; **Fig 2Q**).

Discussion

Loss of Vangl2 function, whether via the semidominant *Lp* missense mutation or a targeted knockout, leads to decreased dendrite arbor complexity, spine maturity and glutamatergic synapse density without similar losses in GABAergic synapse density on forebrain pyramidal neuron dendrites. As dendritic spines are the specific subcellular site of glutamatergic synapses in pyramidal neurons, these data are consistent with previous findings that Vangl2 localizes to the postsynaptic compartment of glutamatergic synapses, where it interacts with PSD95, trans-synaptic adhesion molecules and the PCP pathway protein Prickle2 [14-16]. Our genetic data corroborate previous reports of similar phenotypes following shRNA-mediated knockdown of Vangl2 in cultured neurons [15, 33] and have allowed us to compare and contrast neurodevelopmental phenotypes induced by two molecularly distinct (engineered *null vs.* spontaneous missense) alleles at this locus.

Unlike the *KO* (*null*) allele, the *Lp* allele of *Vangl2* is not a simple loss-of-function: it causes dominant phenotypes to varying degrees in different biological contexts and exerts complex cell biological and biochemical effects on the encoded protein [12, 26, 27, 34]. Unlike homozygous *Vangl2KO* neurons, *Lp* neurons do not have reductions in spine density and their dendrite complexity and glutamatergic synapse phenotypes are not rescued by recombinant overexpression of Vangl2; this suggests that Vangl2 has a molecularly distinct role in spine formation and maturation compared to dendrite arborization and glutamatergic synapse formation. The differences in rescue of these *Lp* neurodevelopmental phenotypes cannot be explained by different temporal requirements for Vangl2 in these subneuronal compartments and processes, because recombinant expression of Vangl2 in the same manner rescues all four phenotypes (dendrite complexity, spine number, spine maturity and glutamatergic synapse density) in *Vangl2$^{-/-}$* neurons.

Conclusions

PCP Pathway Proteins play Important Divergent Roles in Neurons

Genetically altering Vangl2 function, whether by semidominant missense (*Vangl2^{Lp})* or engineered knock-out (*Vangl2KO*), results in forebrain pyramidal neurons with simpler dendrite arbors, a larger proportion of immature spines and fewer glutamatergic synapses. Genetic disruption of other PCP genes in mammals, including Dvl1 [35] and Dact1 [30], cause similar phenotypes. Given widespread neural expression of Vangl2 and several other PCP genes during prenatal development, postnatal development and in the mature brain, it is plausible that the neural functions of these molecules are

similarly widespread and continuous over the lifespan. In prior work we have demonstrated requirements for the Vangl2 partner Dact1 during dendrite, spine and synapse development in both pyramidal neurons [30] and interneurons of the cerebral cortex [36, 37]. However, mutations in *Vangl2* and *Dact1* that exhibit strong mutual rescue during gastrulation [13] do not exhibit similar reciprocal functional relationships during neurodevelopment, suggesting that the molecular mechanisms underlying these phenotypes differ. Consistent with other studies [15, 38, 39] our genetic work therefore suggests that although components of the PCP pathway play important roles in the nervous system, the molecular pathways by which they function in developing neurons differ substantially from the PCP pathway established in studies of basic embryonic development.

The Goldilocks Principle in Molecular Neuropsychiatry

Evidence increasingly supports that neurodevelopmental and neuroplastic processes regulating spine and glutamatergic synapses contribute to the pathogenesis of psychiatric conditions including autism, schizophrenia and major affective disorders [2-4, 40-43]. In line with this, several PCP proteins that contribute to these processes have been implicated in psychiatric symptomatology and pathophysiology. For example, elimination of Dvl1 reduces social behavior in mice [44] and Prickle2 sequence variants associated with autism lead to dendrite and glutamatergic synapse phenotypes when introduced into mice [45]. Our genetic work with Vangl2 accords with these findings and is of additional translational interest in that it underscores that similar neural phenotypes can be caused by very different molecular defects, and in fact even

78

by functionally-opposite molecular defects, at some genetic loci and in some biochemical pathways. We refer to this as the "Goldilocks Principle" in molecular neuropsychiatry: the dosage principle that either *too much* or *too little* can be deleterious. This is a well-established theme for PCP signaling in other developmental contexts [13, 46, 47]. A similar phenomenon has been observed for loci that contribute to neuropsychiatry through entirely different mechanisms, including ion channel proteins such as KCNA2 for which both gain- and loss-of-function mutations cause epilepsy [48] and CACNA1C for which both a gain-of-function mutation and reduced expression variants are associated with bipolar disorder [49]. This is also now firmly established for several copy number variants, such as7q11.23 and 22q11.2, that contribute to psychiatric susceptibility either when deleted or duplicated [3, 50].
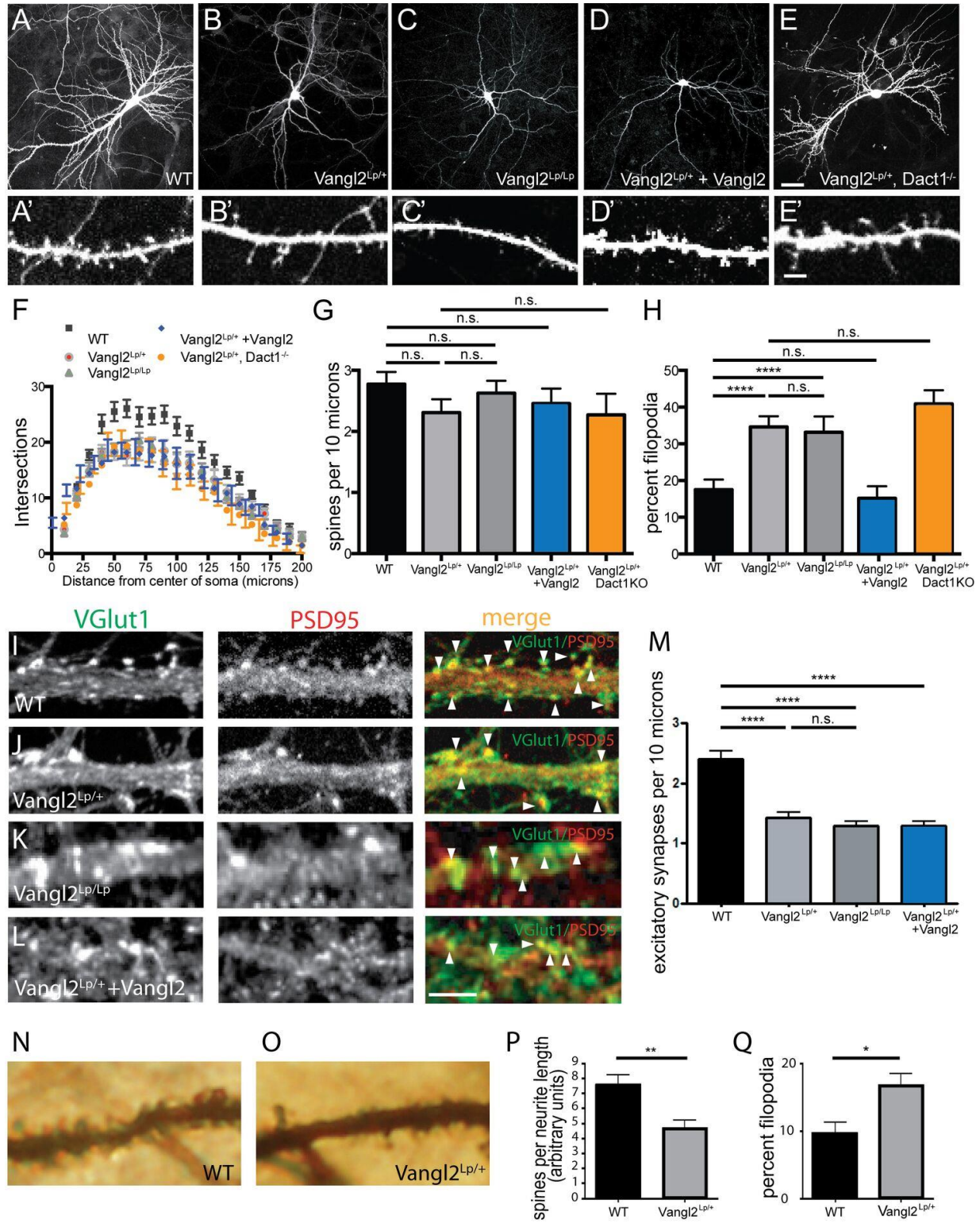
Figure 3.1
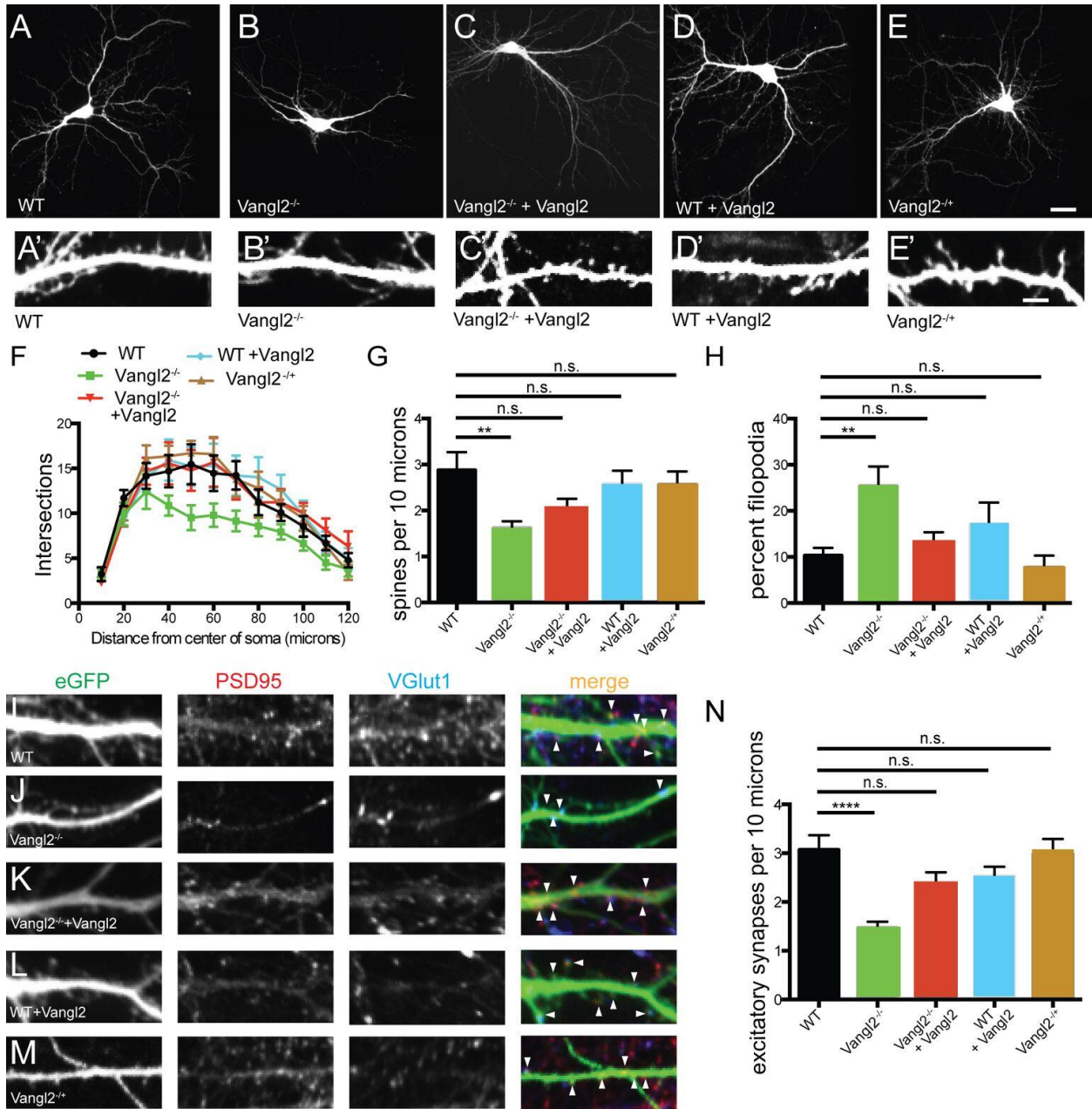
FIGURE LEGENDS

Figure 3.1. Differentiation phenotypes in cultured *Vangl2KO* forebrain neurons. **A-E** EGFP-transfected cultured forebrain neurons from WT (**A**), Vangl2$^{-/-}$ (**B**), Vangl2$^{-/-}$ +Vangl2 (**C**), WT+ Vangl2 (**D**), Vangl2 $^{-/+}$ (**E**). **A'-E'** corresponding dendritic segments at higher magnification. **F-H** Vangl2$^{-/-}$ neurons have simpler dendritic arbors as quantified by Sholl analysis (**F**), fewer dendritic spines (**G**), and less mature spines (**H**) than controls. **I-M** Immunostaining for glutamatergic synapse markers along dendrite segments from WT (**I**), Vangl2$^{-/-}$ (**J**), Vangl2$^{-/-}$+Vangl2 (**K**), WT+ Vangl2 (**L**) and Vangl2 $^{-/+}$ (**M**) neurons. **N** Quantification. n.s.=p>0.05, **p≤0.01, ****p≤0.0001.

Figure 3.2

Figure 3.2. Differentiation phenotypes in *Vangl2^{Lp}* forebrain neurons. **A-E** EGFP-transfected cultured neurons from WT (**A**), *Vangl2$^{Lp/+}$* (**B**), *Vangl2$^{Lp/Lp}$* (**C**), *Vangl2$^{Lp/+}$* + Vangl2 (**D**), *Vangl2$^{Lp/+}$*; *Dact1$^{-/-}$* (**E**). **A'-E'** corresponding dendritic segments at higher magnification. **F-H.** Quantification. *Vangl2^{Lp}* neurons have simpler dendritic arbors (**F**), no reduction in total density of dendritic projections (spines + filipodia) (**G**), but a larger proportion of immature (filopodial) dendritic projections (**H**) than controls; only the last phenotype is rescued by recombinant expression of Vangl2 (blue bar). **I-L** Immunostaining for glutamatergic synapse markers along dendrite segments from WT (**I**), *Vangl2$^{Lp/+}$* (**J**), *Vangl2$^{Lp/Lp}$* (**K**) and *Vangl2$^{Lp/+}$*+*Vangl2* (**L**) cultured neurons. **M** Quantification. **N-O.** Segments of apical dendrite from a Golgi-stained pyramidal neuron in hippocampal CA1 of WT (**N**) and *Vangl2$^{Lp/+}$* (**O**) littermates. Quantification of total spines (**P**) and immature (filopodial) spines (**Q**). Scale bars: 5 µm in **A-E**, **A'-E'**, **I-L**; 10 µm in **N** and **O**. n.s.= $p>0.05$, *$p≤0.05$; **$p≤0.01$, ****$p≤0.0001$.

References

1.	Williams AJ, Umemori H: **The best-laid plans go oft awry: synaptogenic growth factor signaling in neuropsychiatric disease**. *Front Synaptic Neurosci* 2014, **6**:4.
2.	Sekar A, Bialas AR, de Rivera H, Davis A, Hammond TR, Kamitaki N, Tooley K, Presumey J, Baum M, Van Doren V, Genovese G, Rose SA, Handsaker RE, Daly MJ, Carroll MC, Stevens B, McCarroll SA: **Schizophrenia risk from complex variation of complement component 4**. *Nature* 2016.
3.	Pinto D, Delaby E, Merico D, Barbosa M, Merikangas A, Klei L, Thiruvahindrapuram B, Xu X, Ziman R, Wang Z, Vorstman JA, Thompson A, Regan R, Pilorge M, Pellecchia G, Pagnamenta AT, Oliveira B, Marshall CR, Magalhaes TR, Lowe JK, Howe JL, Griswold AJ, Gilbert J, Duketis E, Dombroski BA, De Jonge MV, Cuccaro M, Crawford EL, Correia CT, Conroy J *et al*: **Convergence of genes and cellular pathways dysregulated in autism spectrum disorders**. *Am J Hum Genet* 2014, **94**(5):677-694.
4.	Duman RS: **Pathophysiology of depression and innovative treatments: remodeling glutamatergic synaptic connections**. *Dialogues Clin Neurosci* 2014, **16**(1):11-27.
5.	Sanders SJ: **First glimpses of the neurobiology of autism spectrum disorder**. *Curr Opin Genet Dev* 2015, **33**:80-92.
6.	Ahmad-Annuar A, Ciani L, Simeonidis I, Herreros J, Ben Fredj N, Rosso SB, Hall A, Brickley S, Salinas PC: **Signaling across the synapse: a role for Wnt and Dishevelled in presynaptic assembly and neurotransmitter release**. *Journal of Cell Biology* 2006, **174**(1):127-139.
7.	Cerpa W, Godoy JA, Alfaro I, Farias GG, Metcalfe MJ, Fuentealba R, Bonansco C, Inestrosa NC: **Wnt-7a modulates the synaptic vesicle cycle and synaptic transmission in hippocampal neurons**. *Journal of Biological Chemistry* 2008, **283**(9):5918-5927.
8.	Farias GG, Valles AS, Colombres M, Godoy JA, Toledo EM, Lukas RJ, Barrantes FJ, Inestrosa NC: **Wnt-7a Induces Presynaptic Colocalization of a7-Nicotinic Acetylcholine Receptors and Adenomatous Polyposis Coli in Hippocampal Neurons**. *Journal of Neuroscience* 2007, **27**(20):5313-5325.
9.	Okerlund ND, Cheyette BN: **Synaptic Wnt signaling-a contributor to major psychiatric disorders?** *J Neurodev Disord* 2011, **3**(2):162-174.
10.	Farias GG, Alfaro I, Cerpa W, Grabowski CP, Godoy JA, Bonansco C, Inestrosa NC: **Wnt-5a/JNK signaling promotes the clustering of PSD-95 in hippocampal neurons**. *Journal of Biological Chemistry* 2009.
11.	Varela-Nallar L, Alfaro IE, Serrano FG, Parodi J, Inestrosa NC: **Wingless-type family member 5a (Wnt-5a) stimulates synaptic differentiation and function of glutamatergic synapses**. *Proceedings of the National Academy of Science* 2010, **107**(49):21164-21169.
12.	Torban E, Wang HJ, Groulx N, Gros P: **Independent mutations in mouse Vangl2 that cause neural tube defects in looptail mice impair interaction with members of the Dishevelled family**. *J Biol Chem* 2004, **279**(50):52703-52713.

13. Suriben R, Kivimae S, Fisher DA, Moon RT, Cheyette BNR: **Posterior malformations in Dact1 mutant mice arise through misregulated Vangl2 at the primitive streak.** *Nature Genetics* 2009, **41**(9):977-985.
14. Yoshioka T, Hagiwara A, Hida Y, Ohtsuka T: **Vangl2, the planar cell polarity protein, is complexed with postsynaptic density protein PSD-95 [corrected]**. *FEBS Lett* 2013, **587**(10):1453-1459.
15. Nagaoka T, Ohashi R, Inutsuka A, Sakai S, Fujisawa N, Yokoyama M, Huang YH, Igarashi M, Kishi M: **The Wnt/planar cell polarity pathway component Vangl2 induces synapse formation through direct control of N-cadherin**. *Cell Rep* 2014, **6**(5):916-927.
16. Nagaoka T, Tabuchi K, Kishi M: **PDZ interaction of Vangl2 links PSD-95 and Prickle2 but plays only a limited role in the synaptic localisation of Vangl2**. *Sci Rep* 2015, **5**:12916.
17. Phillips HM, Murdoch JN, Chaudhry B, Copp AJ, Henderson DJ: **Vangl2 Acts via RhoA Signaling to Regulate Polarized Cell Movement During Development of the Proximal Outflow Tract**. *Circulation Research* 2009, **96**:292-299.
18. Lindqvist M, Horn Z, Bryja V, Schulte G, Papachristou P, Ajime R, Dyberg C, Arenas E, Yamaguchi TP, Lagercrantz H, Ringstedt T: **Vang-like Protein 2 and Rac1 Interact to Regulate Adherens Junctions**. *Journal of Cell Science* 2009, **123**:472-483.
19. Nakayama AY, Harms MB, Luo L: **Small GTPases Rac and Rho in the Maintenance of Dendritic Spines and Branches in Hippocampal Pyramidal Neurons**. *Journal of Neuroscience* 2000, **20**(14):5329-5338.
20. Negishi M, Katoh H: **Rho Family GTPases and Dendrite Plasticity**. *The Neuroscientist* 2005, **11**(3):187-191.
21. Tashiro A, Minden A, Yuste R: **Regulation of dendritic spine morphology by the Rho family of small GTPases: Antagonistic roles of Rac and Rho**. *Cerebral Cortex* 2000, **10**(10):927-938.
22. Van Aelst L, Cline HT: **Rho GTPases and activity-dependent dendrite development**. *Current Opinion in Neurobiology* 2004, **2004**(14).
23. Kibar Z, Vogan KJ, Groulx N, Justice MJ, Underhill DA, Gros P: **Ltap, a mammalian homolog of Drosophila Strabismus/Van Gogh, is altered in the mouse neural tube mutant Loop-tail**. *Nat Genet* 2001, **28**(3):251-255.
24. Strong LC, Hollander WF: **Hereditary loop-tail in the house mouse**. *Journal of Heredity* 1947, **40**:329-334.
25. Murdoch JN, Doudney K, Paternotte C, Copp AJ, Stanier P: **Severe neural tube defects in the loop-tail mouse result from mutation of Lpp1, a novel gene involved in floor plate specification**. *Hum Mol Genet* 2001, **10**(22):2593-2601.
26. Song H, Hu J, Chen W, Elliott G, Andre P, Gao B, Yang Y: **Planar cell polarity breaks bilateral symmetry by controlling ciliary positioning**. *Nature* 2010, **466**(7304):378-382.
27. Yin H, Copley CO, Goodrich LV, Deans MR: **Comparison of phenotypes between different vangl2 mutants demonstrates dominant effects of the Looptail mutation during hair cell development**. *PLoS One* 2012, **7**(2):e31988.

28. Kivimae S, Yang XY, Cheyette BNR: **All Dact (Dapper/Frodo) scaffold proteins dimerize and exhibit conserved interactions with Vangl, Dvl, and serine/threonine kinases**. *BMC Biochemistry* 2011, **12(1):33**:[Epub].

29. Elia LP, Yamamoto M, Zang K, Reichardt LF: **p120 Catenin regulates dendritic spine and synapse development through Rho-family GTPases and cadherins**. *Neuron* 2006(51):43-56.

30. Okerlund ND, Kivimae S, Tong CK, Peng I-F, Ullian EM, Cheyette BNR: **Dact1 Is a Postsynaptic Protein Required for Dendrite, Spine, and Excitatory Synapse Development in the Mouse Forebrain**. *Journal of Neuroscience* 2010, **30**(12):4362-4368.

31. Banker G, Goslin K (eds.): **Culturing Nerve Cells**, 2nd edn. Cambridge, Massachusetts: The MIT Press; 1998.

32. Lake BB, Sokol SY: **Strabismus regulates asymmetric cell divisions and cell fate determination in the mouse brain**. *Journal of Cell Biology* 2009, **185**(1):59-66.

33. Hagiwara A, Yasumura M, Hida Y, Inoue E, Ohtsuka T: **The planar cell polarity protein Vangl2 bidirectionally regulates dendritic branching in cultured hippocampal neurons**. *Mol Brain* 2014, **7**:79.

34. Gravel M, Iliescu A, Horth C, Apuzzo S, Gros P: **Molecular and cellular mechanisms underlying neural tube defects in the loop-tail mutant mouse**. *Biochemistry* 2010, **49**(16):3445-3455.

35. Rosso SB, Sussman DJ, Wynshaw-Boris A, Salinas PC: **Wnt signalling through Dishevelled, Rac and Jnk regulates dendritic development.** *Nature Neuroscience* 2005, **8**(1):34-42.

36. Arguello A, Yang X, Vogt D, Stanco A, Rubenstein JL, Cheyette BN: **Dapper antagonist of catenin-1 cooperates with Dishevelled-1 during postsynaptic development in mouse forebrain GABAergic interneurons**. *PLoS One* 2013, **8**(6):e67679.

37. Arguello A, Cheyette BN: **Dapper Antagonist of Catenin-1 (Dact1) contributes to dendrite arborization in forebrain cortical interneurons**. *Commun Integr Biol* 2014, **6**(6):e26656.

38. Glasco DM, Sittaramane V, Bryant W, Fritzsch B, Sawant A, Paudyal A, Stewart M, Andre P, Cadete Vilhais-Neto G, Yang Y, Song MR, Murdoch JN, Chandrasekhar A: **The mouse Wnt/PCP protein Vangl2 is necessary for migration of facial branchiomotor neurons, and functions independently of Dishevelled**. *Dev Biol* 2012, **369**(2):211-222.

39. Qu Y, Huang Y, Feng J, Alvarez-Bolado G, Grove EA, Yang Y, Tissir F, Zhou L, Goffinet AM: **Genetic evidence that Celsr3 and Celsr2, together with Fzd3, regulate forebrain wiring in a Vangl-independent manner**. *Proc Natl Acad Sci U S A* 2014, **111**(29):E2996-3004.

40. Krumm N, O'Roak BJ, Shendure J, Eichler EE: **A de novo convergence of autism genetics and molecular neuroscience**. *Trends Neurosci* 2014, **37**(2):95-105.

41. De Rubeis S, He X, Goldberg AP, Poultney CS, Samocha KE, Cicek AE, Kou Y, Liu L, Fromer M, Walker EM, Singh T, Klei L, Kosmicki J, Fu S-C: **Synaptic, transcriptional and chromatin genes disrupted in autism**. *Nature* 2014.

42. Musazzi L, Treccani G, Mallei A, Popoli M: **The action of antidepressants on the glutamate system: regulation of glutamate release and glutamate receptors**. *Biol Psychiatry* 2013, **73**(12):1180-1188.

43. Yi F, Danko T, Botelho SC, Patzke C, Pak C, Wernig M, Sudhof TC: **Autism-associated SHANK3 haploinsufficiency causes Ih channelopathy in human neurons**. *Science* 2016.

44. Long JM, LaPorte P, Paylor R, Wynshaw-Boris A: **Expanded characterization of the social interaction abnormalities in mice lacking Dvl1**. *Genes Brain Behav* 2004, **3**(1):51-62.

45. Sowers LP, Loo L, Wu Y, Campbell E, Ulrich JD, Wu S, Paemka L, Wassink T, Meyer K, Bing X, El-Shanti H, Usachev YM, Ueno N, Manak JR, Shepherd AJ, Ferguson PJ, Darbro BW, Richerson GB, Mohapatra DP, Wemmie JA, Bassuk AG: **Disruption of the non-canonical Wnt gene PRICKLE2 leads to autism-like behaviors with evidence for hippocampal synaptic dysfunction**. *Mol Psychiatry* 2013, **18**(10):1077-1089.

46. Park E, Kim GH, Choi SC, Han JK: **Role of PKA as a negative regulator of PCP signaling pathway during Xenopus gastrulation movements**. *Dev Biol* 2006, **292**(2):344-357.

47. Veeman MT, Slusarski DC, Kaykas A, Louie SH, Moon RT: **Zebrafish prickle, a modulator of noncanonical Wnt/Fz signaling, regulates gastrulation movements**. *Curr Biol* 2003, **13**(8):680-685.

48. Syrbe S, Hedrich UB, Riesch E, Djemie T, Muller S, Moller RS, Maher B, Hernandez-Hernandez L, Synofzik M, Caglayan HS, Arslan M, Serratosa JM, Nothnagel M, May P, Krause R, Loffler H, Detert K, Dorn T, Vogt H, Kramer G, Schols L, Mullis PE, Linnankivi T, Lehesjoki AE, Sterbova K, Craiu DC, Hoffman-Zacharska D, Korff CM, Weber YG, Steinlin M *et al*: **De novo loss- or gain-of-function mutations in KCNA2 cause epileptic encephalopathy**. *Nat Genet* 2015, **47**(4):393-399.

49. Gershon ES, Grennan K, Busnello J, Badner JA, Ovsiew F, Memon S, Alliey-Rodriguez N, Cooper J, Romanos B, Liu C: **A rare mutation of CACNA1C in a patient with bipolar disorder, and decreased gene expression associated with a bipolar-associated common SNP of CACNA1C in brain**. *Mol Psychiatry* 2014, **19**(8):890-894.

50. Sanders SJ, He X, Willsey AJ, Ercan-Sencicek AG, Samocha KE, Cicek AE, Murtha MT, Bal VH, Bishop SL, Dong S, Goldberg AP, Jinlu C, Keaney JF, 3rd, Klei L, Mandell JD, Moreno-De-Luca D, Poultney CS, Robinson EB, Smith L, Solli-Nowlan T, Su MY, Teran NA, Walker MF, Werling DM, Beaudet AL, Cantor RM, Fombonne E, Geschwind DH, Grice DE, Lord C *et al*: **Insights into Autism Spectrum Disorder Genomic Architecture and Biology from 71 Risk Loci**. *Neuron* 2015, **87**(6):1215-1233.

Publishing Agreement

It is the policy of the University to encourage the distribution of all theses, dissertations, and manuscripts. Copies of all UCSF theses, dissertations, and manuscripts will be routed to the library via the Graduate Division. The library will make all theses, dissertations, and manuscripts accessible to the public and will preserve these to the best of their abilities, in perpetuity.

Please sign the following statement:

I hereby grant permission to the Graduate Division of the University of California, San Francisco to release copies of my thesis, dissertation, or manuscript to the Campus Library to provide access and preservation, in whole or in part, in perpetuity.

Author Signature   Date   9/2/16